taxonomy

MDPI

Article

Comparative Morphology, Phylogeny, Classification and Evolution of Interstitial Habits in Microcambevine Catfishes (Siluriformes: Trichomycteridae)

Wilson J. E. M. Costa * and Axel M. Katz

Laboratory of Systematics and Evolution of Teleost Fishes, Institute of Biology, Federal University of Rio de Janeiro, Caixa Postal 68049, Rio de Janeiro CEP 21941-971, Brazil; axelmk@gmail.com

* Correspondence: wcosta@acd.ufrj.br

Abstract: The Microcambevinae are a catfish subfamily endemic to the Brazilian Atlantic Forest, comprising rare species with interstitial habits. Microcambevines have been classified in two genera, *Listrura* and *Microcambeva*, but the relationships among included intrageneric lineages are still poorly understood. The objectives of this study are to conduct a phylogenetic analysis integrating morphological characters and a multigene dataset, and to propose a classification better reflecting morphological diversity and phylogenetic relationships. Phylogenetic analyses combining 57 morphological characters and a 2563 bp molecular dataset generated similar phylogenetic trees with high support values for most clades, including the two genera and some intrageneric groups. Six morphologically distinctive infrageneric lineages, three in *Listrura* and three in *Microcambeva*, are classified as subgenera, as well as two new species are described. The morphological diversity here recorded integrated to available information about habitat indicate high level of divergent specialisation among lineages. The analyses indicate a series of convergent morphological traits between *Listrura* and other teleosts sharing a fossorial lifestyle, as well as specialised traits independently occurring within *Listrura* lineages. Similarly, a great diversity of morphological traits occurs convergently in *Microcambeva* lineages and other teleosts sharing psammophilic habits. This study shows that combining molecular and morphological data yields well-supported phylogenies, making possible to unambiguously diagnose clades and to establish evolutionary hypothesis on morphological evolution.

Keywords: Atlantic Forest; fossorial lifestyle; molecular phylogeny; Neotropics; osteology; new subgenera; psammophily

Citation: Costa, W.J.E.M.; Katz, A.M. Comparative Morphology, Phylogeny, Classification and Evolution of Interstitial Habits in Microcambevine Catfishes (Siluriformes: Trichomycteridae). *Taxonomy* **2021**, *1*, 313–344. https://doi.org/10.3390/taxonomy1040025

Academic Editor: Mathias Harzhauser

Received: 3 October 2021
Accepted: 9 November 2021
Published: 11 November 2021

1. Introduction

Shallow freshwater aquatic habitats inserted within tropical and subtropical forests shelter a diverse fauna of small teleost fishes, often exhibiting numerous morphological and behavioural adaptations to live in special habitats [1]. In the South American Atlantic Forest, considered among the five main biodiversity hotspots in the world [2], the presence of a such diversified and specialised ichthyofauna has been intensively documented in recent years, including the discovery of fish groups almost entirely unknown. This is the case of the Microcambevinae, a trichomycterid catfish subfamily endemic to the Atlantic Forest, comprising small and rare species with interstitial habits [3], of which all except one were described after 1988.

Despite the relatively high morphological diversity, microcambevines have been classified in only two genera, *Listrura* de Pinna, 1988 and *Microcambeva* Costa & Bockmann, 1993 [3]. Due to the superficial morphological similarity between species of *Listrura* and species of the Amazon subfamily Glanapteryginae, including an elongate body, a minute eye, and rudimentary or absent fins, *Listrura* was formerly placed in this subfamily [4]. Similarly, *Microcambeva* was first placed in the Amazon subfamily Sarcoglanidinae, by

Microcambeva sharing several morphological features with sarcoglanidines, including the presence of a long maxillary bone, a small ossification anteriorly attached to the autopalatine, and a small, paired barbel-like structure on the branchiostegal region [5]. Only recently, Costa et al. [3] recognised Microcambevinae as a separate subfamily, sister to a clade comprising both Glanapteryginae and Sarcoglanidinae, as well as other three predominantly Amazon subfamilies, the Stegophilinae, Tridentinae and Vandelliinae. All these six families together are informally known as the TSVSGM-clade, referring to the initial letters of each included subfamily [3,6]. However, relationships among intrageneric groups of the Microcambevinae are still poorly understood. The first objective of the present paper is to perform a comparative morphological analysis searching for characters potentially informative to diagnose intra-subfamilial clades and divergent lineages, and to conduct a phylogenetic analysis integrating morphological characters and a multigene dataset.

History of Microcambevine Taxonomy

Listrura was diagnosed by de Pinna [4] based on a combination of character states of the external morphology, as well as a few osteological character states taken from the type species, *L. nematopteryx* de Pinna, 1988. This species has a very elongate eel-shaped body and a pectoral fin comprising a barbel-like structure with a single long ray. The first specimens of the type series were collected during a field inventory (1983–1986) directed to search annual killifishes (Cyprinodontiformes: Rivulidae) in swampy areas of the Rio de Janeiro state coastal plains, coordinated by one of us (WJEMC). A great concentration of specimens has been found in a small swamp with a deep layer of black mud, above which was a narrow layer of leaf litter and amphibious plants, with the water surface at only about 1 cm above the leaf litter; in this habitat, specimens were buried in the muddy bottom, between about one and ten centimetres deep (WJEMC personal observations, 1984, 1992). A few other specimens were found in the leaf litter deposits close to the margin of an adjacent shallow stream. Another species, *Eremophilus camposi* Miranda Ribeiro, 1957 from the Rio Ribeira de Iguape basin, having the pectoral fin with a shorter first ray, followed by two rudimentary rays, and then known from a single specimen, was also included in *Listrura* by de Pinna [4] on the basis of the similarity of some external morphological features.

During the early 1990s, three other *Listrura*-like species were first collected by the Laboratory of Amphibia team (Institute of Biology, UFRJ), coordinated by Sergio Potsch, and donated to one of us (WJEMC) for study. One species, similar to *L. nematopteryx* and later described as *L. picinguabae* Villa-Verde & Costa, 2006, was collected in the coastal plains of São Paulo state, south-eastern Brazil [7]. Between 1992 and 1996, this species was known from only five specimens sporadically collected in leaf litter deposits close to the stream bank (WJEMC personal observation 1994), but in 1996, a great concentration of specimens was collected in a shallow muddy swampy covered by a dense layer of leaf litter, about five meters from the stream margin (WJEMC personal observation 1996), indicating that the preferential habitat of *L. picinguabae* is similar to that of *L. nematopteryx*. The second species of *Listrura* found in that period, later described as *L. tetraradiata* Landim & Costa, 2004, has a distinct general morphology [8], as well as it was collected in a different habitat from that above described for *L. nematopteryx*. The body of *L. tetraradiata* is not so elongated as in other congeners, and it has a well-developed pectoral fin [8]. *Listrura tetraradiata* inhabits a shallow stream, with a high concentration of specimens found superficially buried in the bottom leaf litter at the edge of a dam, at about 40 cm deep, where some specimens could be eventually observed swimming just above the leaf litter (WJEMC personal observation 1995). The third species, similar to *L. camposi*, was collected in leaf litter deposits close to the stream bank, in the Santa Catarina Island, southern Brazil, and is still today undescribed (*Listrura* sp. 1 in the present analysis). In more recent years, other species morphologically similar to *L. nematopteryx* (*L. costai* Villa-Verde, Lazzarotto & Lima, 2012 and three still undescribed species, among which two are herein described) and to *L. camposi* (*L. boticario*

de Pinna & Wosiacki, 2002 and *L. depinnai* Villa-Verde, Ferrer & Malabarba, 2013) were found in field studies [9–11].

Microcambeva was diagnosed by a combination of morphological character states present in its type species, *M. barbata* Costa & Bockmann, 1994, the only species of the genus known at that time [5]. This species is small, not surpassing about 25 mm of standard length (SL) and is found slightly buried in sand stretches of rivers with moderate current [5]. The second species of *Microcambeva* to be described was *M. ribeirae* Costa, Lima & Bizerril, 2004, which highly differs from *M. barbata* by having a broader pectoral fin with a first ray that is shorter than the adjacent rays and a narrower and longer snout [12], besides reaching about twice the maximum size of *M. barbata* (i.e., about 50 mm SL). More recently other species similar to *M. barbata* (*M. draco* Mattos & Lima, 2010, *M. jucuensis* Costa, Katz, Mattos & Pereira, 2019, *M. mucuriensis* Costa, Katz, Mattos & Pereira, 2019, and *M. watu* Medeiros, Sarmento-Soares & Lima, 2021) and another one similar to *M. ribeirae* (*M. bendego* Medeiros, Moreira, de Pinna & Lima, 2020) were described [13–16]. Another species, *M. filamentosa* Costa, Katz & Vilardo, 2020, having a very distinctive morphology (i.e., absence of barbel-like structures on the branchiostegal region, distinctively smaller eyes and longer barbels and pectoral-fin filament), was also recently placed in *Microcambeva* [17].

Available data indicate that the morphological diversity, including both external morphology and osteology, occurring within each microcambevine genus is high, with some included taxa exhibiting highly divergent morphological traits and ecological specializations comparable to that occurring in different genera of other trichomycterid subfamilies [18]. The second objective of this study is to propose a classification better reflecting morphological diversity and phylogenetic relationships among microcambevines.

2. Materials and Methods

2.1. Specimens

Specimens used in this study includes both old collections deposited in the ichthyological collection of the Zoology Department, Institute of Biology, Federal University of Rio de Janeiro, Rio de Janeiro (UFRJ) and recent collections, which were made with small dip nets (40 × 30 cm) during daylight. Collection permits were provided by Instituto Chico Mendes de Conservação da Biodiversidade (ICMBio; permit numbers: 38553 and 26262) and field methods were approved by the Ethics Committee for Animal Use of Federal University of Rio de Janeiro (CEUA-CCS-UFRJ; permit number: 065/18). Most specimens were fixed in 10% formalin for a period of 14 days, and then transferred to 70% ethanol. For molecular analyses, whole specimens were fixed and preserved in 98% ethanol, except for specimens of rare species (i.e., the new species herein described), which after euthanasia had a segment of the muscle of the left side of the caudal peduncle dissected, fixed, and preserved in 98% ethanol, while the whole specimen was fixed in 10% formalin as above described.

2.2. Morphological Data

Morphometric and meristic data were taken according to Costa [19], with modifications proposed by Costa et al. [20]; measurements are presented as percent of standard length (SL), except for those related to head morphology, which are expressed as percent of head length. Fin-ray counts include all elements; in species descriptions, lower case roman numerals indicate unsegmented unbranched rays, upper case numerals indicate segmented unbranched rays, and Arabic numerals indicated segmented branched rays. Vertebra counts include all vertebrae except those participating in the Weberian apparatus; the compound caudal centrum was counted as a single element. Specimens were cleared and stained for bone and cartilage (C&S in lists of specimens) following Taylor and Van Dyke [21]. Osteological characters used in species descriptions are those belonging to structures that herein were found to have informative variability among species of *Listrura*, including the mesethmoidal region, jaw suspensorium, opercular apparatus, and parurohyal. Terminology for bones is according to Costa [18], except for 'proximal radial' and 'cartilaginous proximal radial' of the pectoral fin, herein called 'major proximal radial' and

'minor proximal radial' of the pectoral fin. Osteological illustrations were made using a Stemi SV 6 stereomicroscope (Zeiss, Jena, Germany) equipped with camera lucida. Bone measurements follow Costa and Katz [22]. Cephalic latero-sensory system terminology follows Arratia and Huaquin [23], with modifications proposed by Bockmann et al. [24]. A list of specimens used in the comparative analysis appears in the Appendix A. Morphological characters used in the phylogenetic analysis were those with informative variability among the main microcambevine lineages; therefore, an exhaustive survey of morphological characters at the intrageneric species level is beyond the scope of the present analysis.

2.3. DNA Sequences

Total genomic DNA was extracted from muscle tissues of the caudal peduncle and dorsum, using the DNeasy Blood & Tissue Kit (Qiagen, Hilden, Germany), following the manufacturer's protocol. Amplification of the target DNA fragments, including partial sequences of the nuclear gene recombination activating 2 (RAG2) and partial sequences of two mitochondrial genes, cytochrome *c* oxidase subunit I (COI) and cytochrome *b* (CYTB), was made through the polymerase chain reaction (PCR) method, using the following primers: MHRAG2-F1 and MHRAG2-R1 [25], RAG2 TRICHO F and RAG2 TRICHO R [3]; Cytb Siluri F and Cytb Siluri R [7]; L5698-ASN and H7271-COI [7] and FISHF1 and FISHR1 [26]. Double-stranded PCR amplifications were performed in 60 µL reactions with reagents at the following concentrations: 5× GreenGoTaq Reaction Buffer (Promega, Madison, WI, USA), 3.2 mm MgCl2, 1 µm of each primer, 75 ng of total genomic DNA, 0.2 mm of each dNTP and 1 U of standard Taq polymerase or Promega GoTaq Hot Start polymerase. The thermocycling profile was as follows: initial denaturation for 2–5 min at 94–95 °C; 35 cycles of denaturation for 30 s–1 min at 94–95 °C, annealing for 1 min–90 s at 45.0° for COI and 52.0 °C for CYTB and RAG2, and extension for 1 min–90 s at 72 °C; and terminal extension for 4–8 min at 72°C. In all PCR reactions, negative controls without DNA were used to check contaminations. The PCR products were then purified using the Wizard SV Gel and PCR Clean-Up System (Promega). Sequencing reactions were made using the BigDye Terminator Cycle Sequencing Mix (Applied Biosystems, Walthan, USA). Cycle sequencing reactions were performed in 20 µL reaction volumes containing 4 µL BigDye, 2 µL sequencing buffer 5× (Applied Biosystems), 2 µL of the amplified products (10–40 ng), 2 µL primer and 10 µL deionized water. The thermocycling profile was: (1) 35 cycles of 10 s at 96 °C, 5 s at 54 °C and 4 min at 60 °C. A complete list of species and GenBank accession numbers appears in the Appendix B. Alignment was conducted for each gene set using Clustal W [27] algorithm implemented in MEGA 7.0 [28]; no gap was found in analysed alignments.

2.4. Phylogenetic Analyses

The phylogenetic analyses included microcambevine species with specimens available for morphological analysis and to extract DNA, comprising nine species of *Listrura* (*L. camposi*, *L. costai*, *L. depinnai*, *L. nematopteryx* (type species), *L. picinguabae*, *L. tetraradiata*, two new species herein described, and a still undescribed species from Santa Catarina Island) and five species of *Microcambeva* (*M. barbata* (type species), *M. filamentosa*, *M. jucuensis*, *M. mucuriensis*, and *M. ribeirae*). The analysis also included three species with missing molecular data, but available morphological data (*M. bendengo*, *M. draco*, and *M. watu*), as well as one undescribed species of *Listrura* from the Rio São João basin, with DNA sequences available in GenBank (NCBI), but without available morphological data, except for the absence of dorsal fin and the presence of a single-rayed pectoral fin like that described for *L. nematopteryx* [7]. Therefore, the only known microcambevine not included in the analysis was *L. boticario* due to the unavailability of both morphological and molecular data. Out-group taxa included three species representing other lineages of the TSVSGM-clade: *Homodiaetus anisitsi* Eigenmann & Ward, 1907 (Stegophilinae), *Pygidianops amphioxus* de Pinna & Kirovsky, 2011 (Glanapteryginae), and *Stauroglanis gouldingi* de Pinna, 1989 (Sarcoglanidinae); three species of Trichomycterinae, the sister group of the

TSVSGM-clade [3]: *Ituglanis boitata* Ferrer, Donin & Malabarba, 2015, *Scleronema minutum* (Boulenger, 1891), and *Trichomycterus nigricans* Valenciennes, 1832; and one species of the basal trichomycterid Trichogeninae: *Trichogenes longipinnis* Britski & Ortega, 1983.

Fifty-seven informative characters were obtained from the morphological comparative analysis. The list of characters, formulated according to Sereno [29], is provided in the Appendix C, and the distribution of character states among taxa appears in the data matrix of the Appendix D. In results below, the abbreviation 'chast' means character state that are numbered according to the Appendix C. Morphological characters were combined to the molecular set (total of 2564 bp), which were partitioned according to the codon position for each gene, with morphological data placed in a separate partition. The best-fitting models of molecular evolution for each partition was found using the Bayesian information criterion (BIC) of ModelFinder [30], implemented in IQ-TREE 1.6.11 [31], with partition models described in Chernomor et al. [32]; a list of partitions and their respective models of nucleotide substitution appears in the Appendix E.

The concatenated dataset, total of 2620 characters for 25 taxa, was analysed using IQ-TREE for Maximum Likelihood (ML); the reliability of internal branches was inferred using the Shimodaira-Hasegawa-like procedure support (SH-aLRT) [33], the Bayesian-like transformation of SH-aLRT support (aBayes) [34], and the ultrafast bootstrap support (UFBoot) [35,36] with 1000 replicates, using default parameters implemented in IQ-TREE. The concatenated dataset was also analysed using TNT 1.1 [37] for Maximum Parsimony (MP). The phylogenetic analysis was rooted in the trichogenine *T. longipinnis*. The search for most parsimonious trees was conducted using the 'traditional' search algorithm and setting random taxon-addition replicates to ten, tree bisection–reconnection branch swapping, multitrees in effect, collapsing branches of zero length, characters equally weighted, and a maximum of 1000 trees saved in each replicate. Character states were treated as unordered. Branch support was assessed by bootstrap analysis [38], using a heuristic search with 1000 replicates and the same settings used in the MP search. Unambiguous diagnostic character states for the main lineages of *Trichomycterus* were obtained by character state optimization of the combined analysis tree using TNT 1.1. Due to the high incidence of convergent characters in interstitial fishes (see Discussion below), optimization followed the DELTRAN option.

2.5. Taxonomical Accounts

In lists of material examined, geographical names follow Portuguese terms used in the region, thus avoiding common errors or generalizations when tentatively translating them to English, besides making easier their identification in the field; institution acronyms are: CICCAA, ichthyological collection of the Centre of Agrarian and Environmental Sciences, Federal University of Maranhão, Chapadinha, Brazil; UFRJ, ichthyological collection of the Institute of Biology of the Federal University of Rio de Janeiro, Rio de Janeiro, Brazil. In species lists, the abbreviations mean: C&S, specimens cleared and stained for bone and cartilage; DNA, specimens directly fixed in ethanol; SL, standard length.

3. Results

3.1. Phylogenetic Relationships

The comparative morphological analysis resulted in fifty-seven characters with informative variability (see Appendix C for list of characters and Appendix D for distribution of character states among terminal taxa). The ML and MP analyses generated similar phylogenetic trees with high support values for most clades (Figure 1). The comparative morphological analysis generated a series of new characters useful for diagnosing the genera *Listrura* and *Microcambeva*, as well as for diagnosing six distinctive infrageneric lineages, which in order of to preserve nomenclatural stability, are classified as subgenera instead of new genera (see taxonomic accounts below). Within *Listrura*, these lineages include: a clade from south-eastern Brazil (Figure 2) containing the type species, *L. nematopteryx* and other congeners with barbel-like pectoral fin (i.e., subgenus *Listrura*); *L. tetraradiata*,

also from south-eastern Brazil and sister to the subgenus *Listrura*, but with uniquely distinctive morphology due to a complex combination of primitive and derived character states, herein designated as the type species of a new monotypic subgenus; and a clade from south-eastern and southern Brazil, sister to the two above mentioned subgenera and containing the remaining species of the genus, also combining apomorphic and plesiomorphic features, and below described as a new subgenus (see taxonomic accounts below). The three main morphologically distinctive lineages within *Microcambeva* supported in the analysis (Figure 1) are: a clade from eastern and south-eastern Brazil (Figure 3) containing the type species, *M. barbata*, and other similar small species (maximum adult length about 27 mm SL) with a neomorphic autopalatine ossification (i.e., subgenus *Microcambeva*), and sister to other congeners; *M. filamentosa*, a species from south-eastern Brazil with uniquely distinctive morphology, including a series of unique apomorphic and plesiomorphic character states, recognised as a new subgenus; and a clade with two species from south-eastern Brazil, sister to *M. filamentosa*, and exhibiting unique morphological features, including a robust pectoral fin and a short nasal barbel, and also placed in a new subgenus (see taxonomic accounts below).

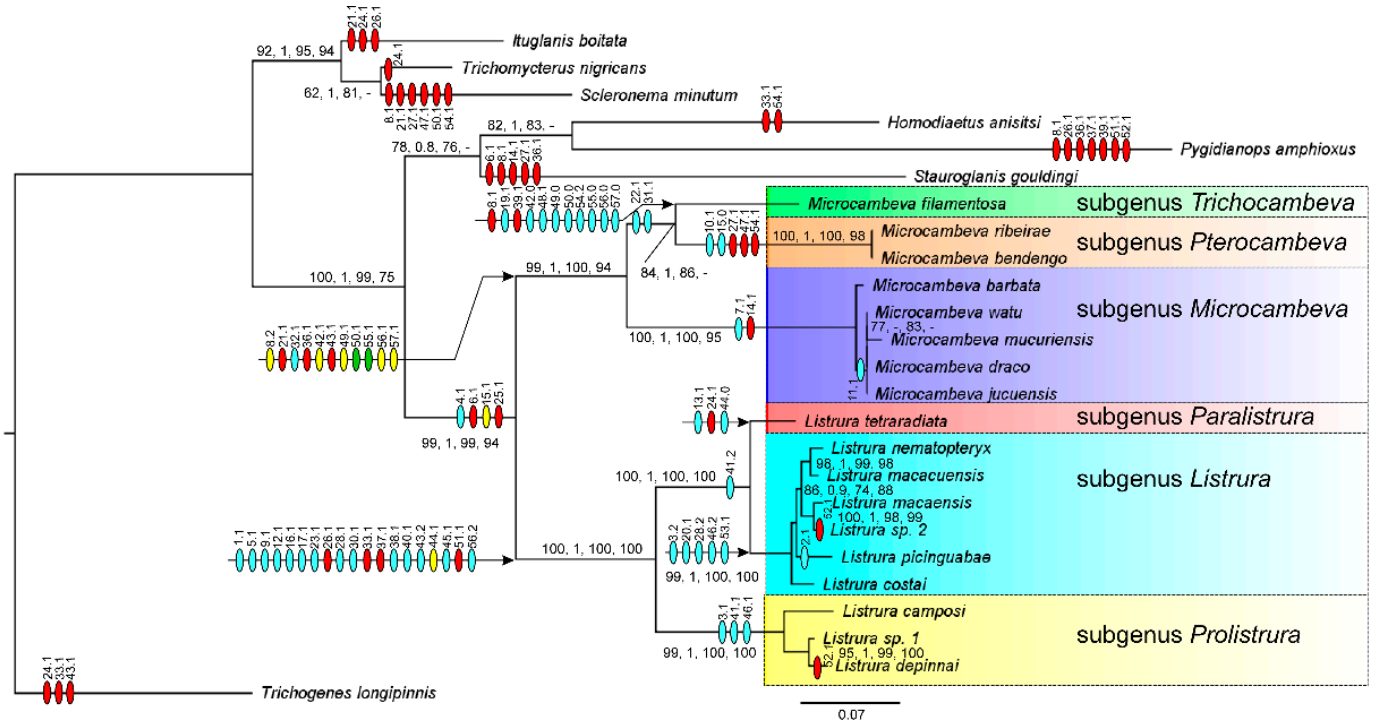

Figure 1. Phylogenetic tree generated by Maximum Likelihood analysis using IQ-TREE for 18 species of the Microcambevinae and seven outgroups, combining three genes (COI, CYTB, and RAG2, with a total of 2563 bp) and 57 osteological characters. Numbers near nodes in horizontal line are support values for phylogenetic analyses, in the following order: Shimodaira-Hasegawa-like procedure support (SH-aLRT) with values above 70%, the Bayesian-like transformation of SH-aLRT support (aBayes) with values above 0.9, and the ultrafast bootstrap support (UFBoot) with values above 70%, for the Maximum Likelihood (ML) analysis, and bootstrap values above 70% for the Maximum Parsimony (MP) analysis. Numbers near nodes vertically written are morphological characters followed by the respective character state after dot, numbered according to the Appendix C; symbol colours below numbers mean: light blue, unambiguous synapomorphies; red, apomorphic character states independently acquired in different analysed taxa; yellow, synapomorphies followed by reversals inside the clade; green, apomorphic character states independently acquired in different analysed taxa, followed by reversals inside the clade.

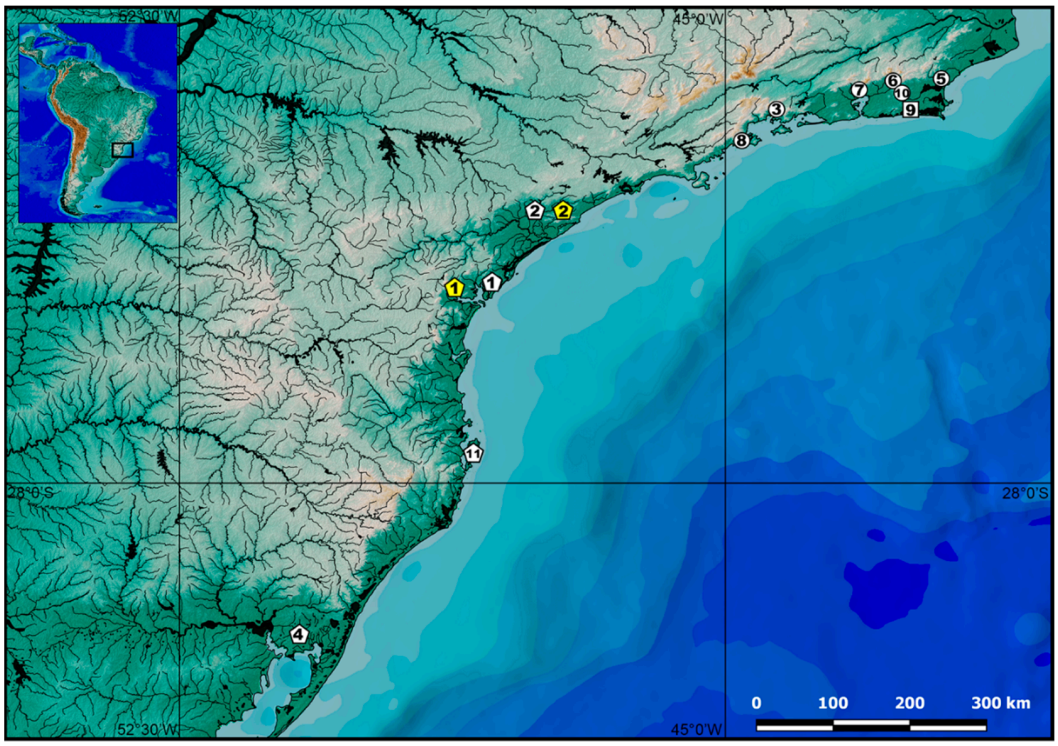

Figure 2. Geographical distribution of species of the genus *Listrura*. Circles indicate species of the subgenus *Listrura*; square, species of the subgenus *Paralistrura*; and pentagons, species of the subgenus *Prolistrura*. 1, *L. boticarioi*; 2, *L. camposi*; 3, *L. costai*; 4, *L. depinnai*; 5, *L. macaensis* sp. nov.; 6, *L. macacuensis* sp. nov.; 7, *L. nematopteryx*; 8, *L. picinguabae*; 9, *L. tetraradiata*; 10, *Listrura* sp. 2; 11, *Listrura* sp. 1. White symbols are type localities.

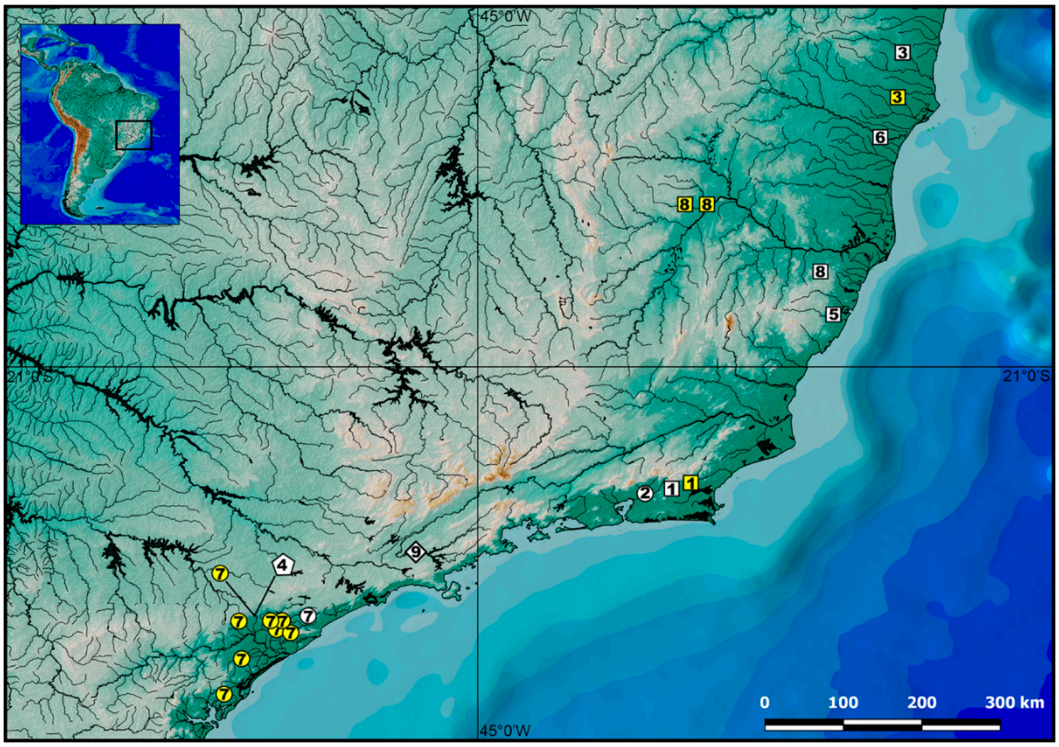

Figure 3. Geographical distribution of species of the genus *Microcambeva* and the incertae sedis microcambevine *Pygidium triguttatum* (lozenge). Circles indicate species of the subgenus *Pterocambeva*; squares, species of the subgenus *Microcambeva*; and pentagon, species of the subgenus *Trichocambeva*. 1, *M. barbata*; 2, *M. bendego*; 3, *M. draco*; 4, *M. filamentosa*; 5, *M. jucuensis*; 6, *M. mucuriensis*; 7, *M. ribeirae*; 8, *M. watu*; 9, *P. triguttatum*. White symbols are type localities.

3.2. Taxonomic Accounts

3.2.1. *Listrura* de Pinna, 1988

Listrura de Pinna, 1988: 114 (type species *Listrura nematopteryx* de Pinna, 1988 by original designation).

Diagnosis. The genus *Listrura* differs from the only other microcambevine genus, *Microcambeva*, by the following apomorphic character states: presence of a lateral widening in the mesethmoid, between anterior cornua and lateral ethmoid (chast.1.1; Figure 4A–D; vs. absence, Figure 4E–H), presence of a short vomer without a posterior process (chast.5.1, Figure 5D; vs. never so short, with a posterior process, Figure 5E), presence of a broad autopalatine without a distinctive postero-lateral process (chast.9.1., Figure 4A–D; vs. autopalatine slender, with a distinctive postero-lateral process, Figure 4E–H), presence of a narrow and flat ossification, postero-medially directed, on the postero-medial margin of the autopalatine (chast.12.1; Figure 4A–D; vs. never a similar process, Figure 4E–H), a comma-shaped antorbital, with a sub-rectangular body and a narrow posterior process (chast.16.1, Figure 4A–D; vs. antorbital never similarly shaped, Figure 4E–H), a rudimentary supraorbital (chast.17.1, Figure 4A–D; vs. well-developed sesamoid supraorbital, Figure 4E–H), a constriction on the interopercle above the odontode patch, yielding a fan-shaped structure (chast.23.1, Figure 4I,J; never a similar interopercle shape, Figure 4K,L), a closed neurocranium roof, without fontanels (chast. 26.1, Figure 5A; vs. opened, with broad fontanel, Figure 5B,C), anterior tip of the frontal reaching at least the area close to the postero-medial corner of the autopalatine (chast.28.1, Figure 4A–D; vs. reaching an area near the autopalatine articular facet for the lateral ethmoid, Figure 4E–H), absence of the median segment of the supraorbital latero-sensory canal, corresponding to the segment between pores s4 and s6 (chast.30.1, Figure 5A; vs. segment present, Figure 5B,C), a weakly or not ossified hypobranchial 3 (chast.33.1, Figure 4M; vs. well-ossified, Figure 4N), an eel-like trunk (chast.37.1, Figure 6A–D; vs. fusiform, Figure 6E–G); the presence of an anterior process on the neural spines of the precaudal vertebrae (chast.38.1, Figure 5F; vs. process absent, Figure 5G), procurrent caudal-fin rays anteriorly extending to an area close to the dorsal and anal fins (chast.40.1; vs. restricted to area adjacent to the caudal fin), dorsal and hypural plates in close proximity, partially or completely ankylosed (chast.41.1–2, Figure 5H,K; vs. with long and broad gap between plates, Figure 5I,J), pectoral girdle slender and thin (chast.45.1, Figure 5L; vs. robust and thick, Figure 5M–O), pelvic fin absent (chast.51.1; vs. present), and a minute eye, its diameter about 7–10% of the head length (chast.56.2; vs. commonly large, about 18–22% of the head length, or moderate about 12–16%). Also distinguished from *Microcambeva* by the following character states: trunk well pigmented (Figure 6A–D; vs. trunk transparent, with a few minute patches of chromatophores, Figure 6E–G), a rounded caudal fin, nearly continuous to the caudal peduncle (Figure 6A–D; vs. bilobed, separated from the caudal peduncle Figure 6E–G), more procurrent caudal-fin rays (21–39 on the dorsal, 21–36 on the ventral part, vs. 5–8 and 5–9, respectively), more vertebrae (43–55 vs. 33–36), a short maxilla, about equal or slightly longer premaxilla length (Figure 4A–D; vs. long, about twice premaxilla length or slightly more, Figure 4E–H), a narrow opercular odontode patch, smaller than the length of the cartilage articulating hyomandibula to the neurocranium (Figure 4I,J; vs. broad, larger than that length, Figure 4K,L), and the absence of a small process on the sub-proximal region of the ceratobranchial 4 (Figure 4M; vs. presence, Figure 4N).

Included taxa. Three subgenera, as below listed.

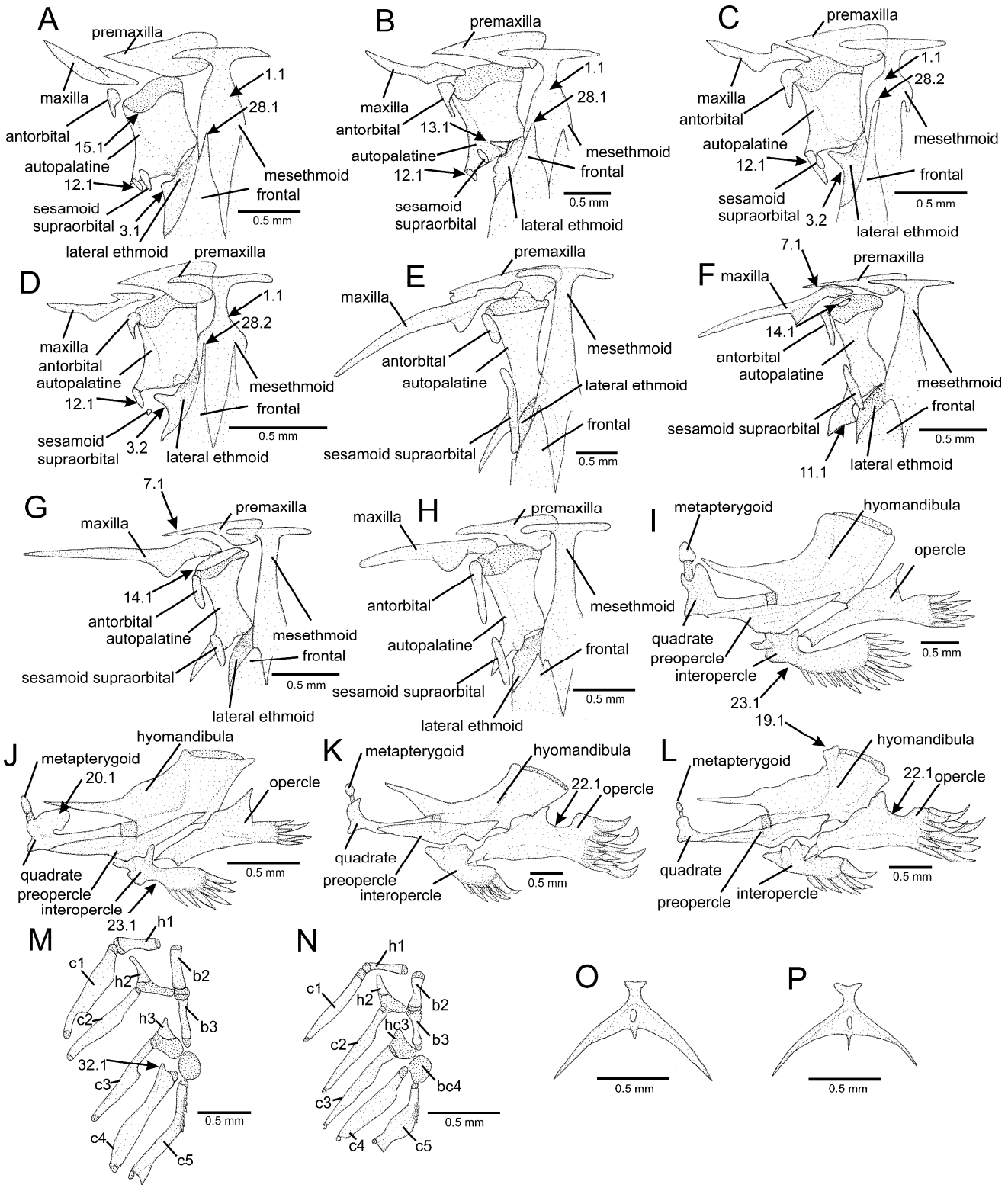

Figure 4. Osteological features in the Microcambevinae: (**A**–**H**) mesethmoidal region and adjacent bones, middle and left portions, dorsal view; (**I**–**L**) left jaw suspensorium and opercular series, lateral view; (**M**,**N**) ventral branchial arch, middle and left portions, dorsal view; (**O**–**P**), parhypural, ventral view, of: (**A**) *Listrura* (*Prolistrura*) *camposi*; (**B**,**I**) *Listrura* (*Paralistrura*) *tetraradiata*; (**C**,**J**,**N**,**O**) *Listrura* (*Listrura*) *macacuensis*; (**D**,**P**) *Listrura* (*Listrura*) *macaensis*; (**E**,**K**) *Microcambeva* (*Pterocambeva*) *ribeirae*; (**F**) *Microcambeva* (*Microcambeva*) *jucuensis*; (**G**) *Microcambeva* (*Microcambeva*) *barbata*; (**H**,**L**,**M**) *Microcambeva* (*Trichocambeva*) *filamentosa*. Larger stippling represents cartilages. The numbers are characters, followed by character states after dots, which are numbered according to Appendix C.

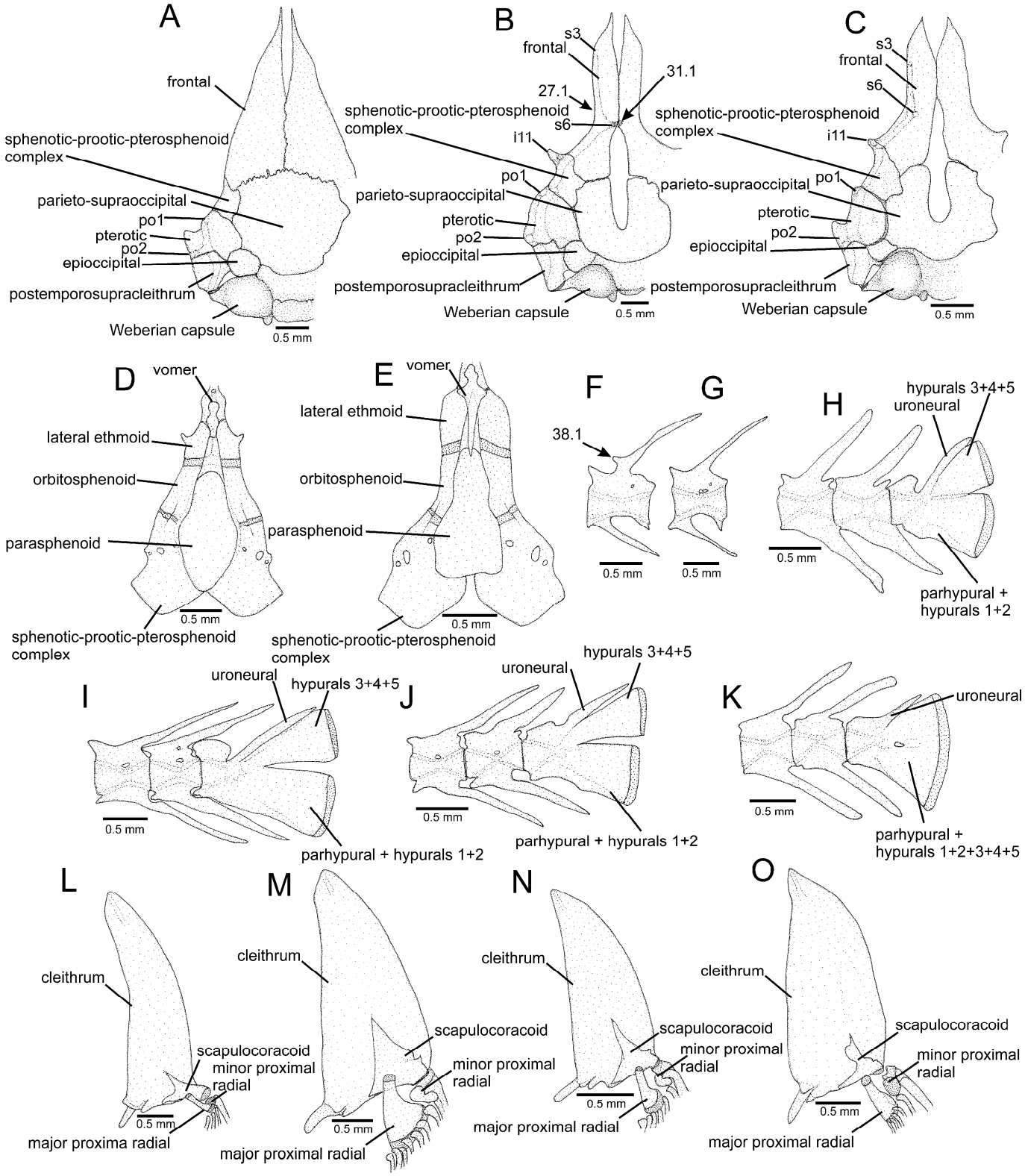

Figure 5. Osteological features in the Microcambevinae: (**A**–**C**) neurocranium, middle and left portions, dorsal view; (**D**,**E**) neurocranium, middle portion, ventral view; (**F**,**G**) nineth free vertebra, left lateral view; (**H**–**K**) caudal skeleton, left lateral view; (**L**–**O**) left shoulder girdle, ventral view, of: (**A**) *Listrura* (*Listrura*) *picinguabae*; (**B**,**G**,**I**,**M**) *Microcambeva* (*Pterocambeva*) *ribeirae*; (**C**,**E**,**N**) *Microcambeva* (*Microcambeva*) *jucuensis*; (**D**,**K**) *Listrura* (*Listrura*) *macacuensis*; (**F**,**H**) *Listrura* (*Prolistrura*) *depinnai*; (**J**,**O**) *Microcambeva* (*Trichocambeva*) *filamentosa*; (**L**) *Listrura* (*Paralistrura*) *tetraradiata*. Larger stippling represents cartilages. The numbers are characters, followed by character states after dots, which are numbered according to Appendix C.

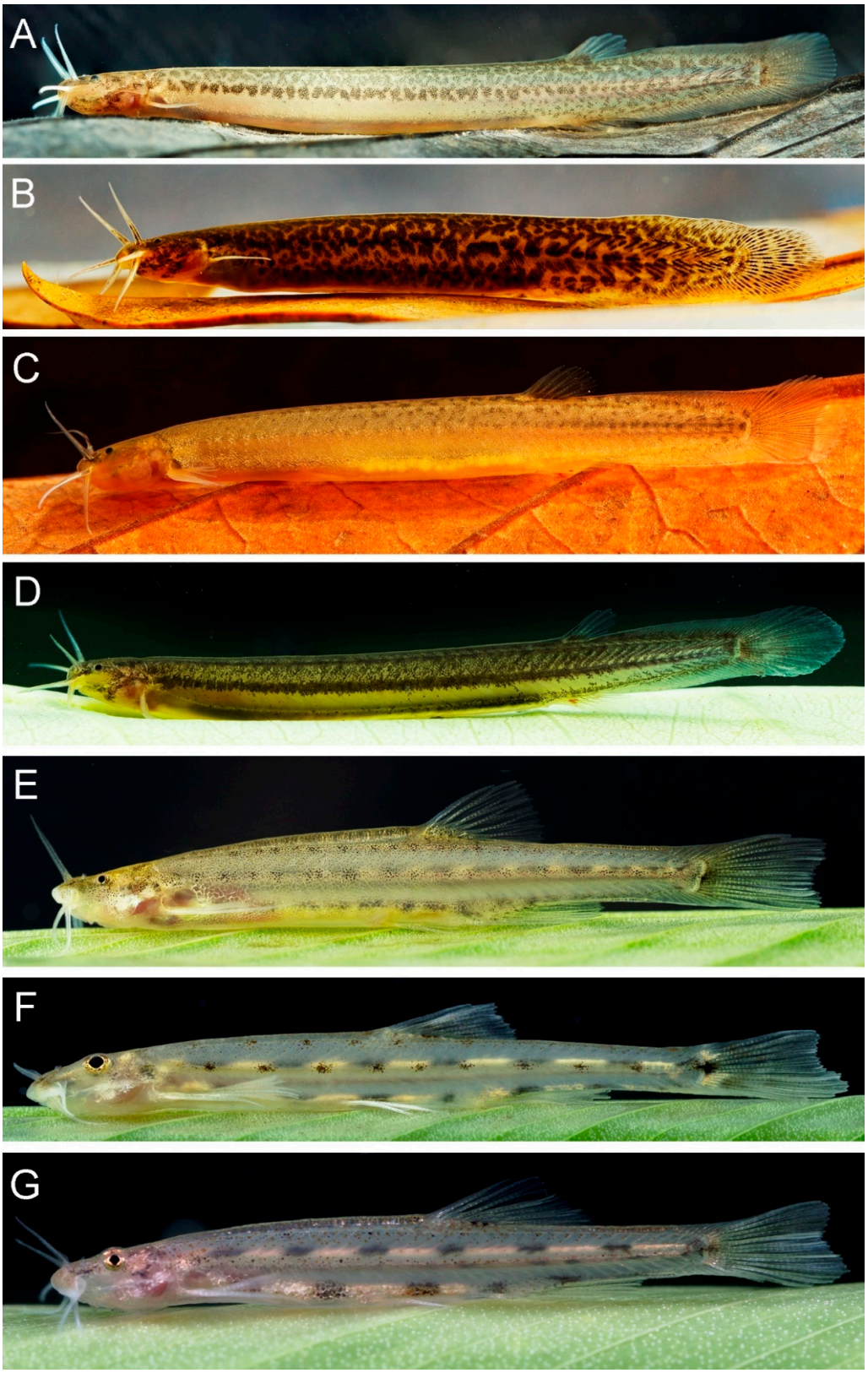

Figure 6. Live specimens of the Microcambevinae, lateral view: (**A**) *Listrura* (*Prolistrura*) *camposi*, UFRJ 11404, 36.4 mm SL; (**B**) *Listrura* (*Prolistrura*) *depinnai*, UFRJ 12552, 33.9 mm SL; (**C**) *Listrura* (*Paralistrura*) *tetraradiata*, UFRJ 11458, 35.1 mm SL; (**D**) *Listrura* (*Listrura*) *macacuensis* sp. nov., UFRJ 12669, holotype, 29.8 mm SL; (**E**) *Microcambeva* (*Trichocambeva*) *filamentosa*, UFRJ 12187, holotype, 31.4 mm SL; (**F**) *Microcambeva* (*Pterocambeva*) *ribeirae*, UFRJ 12189, 33.3 mm SL; (**G**) *Microcambeva* (*Microcambeva*) *barbata*, UFRJ 12185, 20.4 mm SL.

Subgenus *Listrura* de Pinna, 1988

Diagnosis. The subgenus *Listrura* is distinguished from all other subgenera of the genus *Listrura* by the following apomorphic character states: presence of a pronounced subcylindrical process on the lateral margin of the lateral ethmoid (chast.3.2, Figure 4C,D; vs. absence, Figure 4A,B), presence of a laminar extension on the posterior margin of the dorsal process of the quadrate (chast.19.1, Figure 4J; vs. absence, Figure 4I), anterior portion of the frontal long, its tip reaching an area near the autopalatine longitudinal mid-length (chast.28.2, Figure 4C,D; vs. reaching area close to the postero-medial corner of the autopalatine, Figure 4A,B), caudal fin with 11 or 12 principal caudal-fin rays, of which seven or eight are branched (chast.44.1; vs. 13 principal caudal-fin rays, of which nine or ten are branched), a barbel-like pectoral fin, with a single ray (chast.46.2; vs. with two or more rays), and anal-fin origin just anterior or just posterior to dorsal-fin origin, in a vertical anterior to dorsal-fin principal rays (chast.53.1; vs. posterior to dorsal-fin origin, in vertical through dorsal-fin principal rays or posterior to it). The subgenus *Listrura* also differs from *Paralistrura* by the absence of a latero-dorsally directed process on the postero-medial margin of the autopalatine (vs. presence, Figure 4B), by having a short interopercular odontode patch, its length about equal or smaller than the opercular odontode patch (Figure 4J; vs. about twice larger, Figure 4I), fewer teeth in the premaxilla (15–23 vs. 27–32) and dentary (13–21 vs. 24–31), and more vertebrae (49–55 vs. 43–45); and from *Prolistrura* by having dorsal and ventral hypurals plates ankylosed, without a posterior gap, but often with a remnant antero-middle notch (Figure 5K; vs. in close proximity or united, but always keeping a longitudinal middle groove and a posterior gap, Figure 5H).

Included taxa. Three nominal species, *L. costai*, *L. nematopteryx*, and *L. picinguabae*, and three new species, of which two are below described.

Distribution. Coastal plains of south-eastern Brazil, between the Rio Macaé and Rio da Fazenda basins (Figure 2).

Listrura macaensis sp. nov.

LSID: urn:lsid:zoobank.org:act:42BAC952-365B-481F-ABEA-2F5B54A5F7D0.
Figure 7; Table 1.

Figure 7. *Listrura macaensis* sp. nov., UFRJ 12667, holotype, 42.7 mm SL.

Table 1. Morphometric data of *Listrura macaensis* sp. nov.

	Holotype	Paratypes (n = 5)
Standard length (SL)	42.7	25.5–31.7
Percentage of standard length		
Body depth	8.0	7.0–8.9
Caudal peduncle depth	7.5	6.8–9.2
Body width	4.0	3.2–4.5
Caudal peduncle width	2.1	1.4–2.2
Dorsal-fin base length	4.4	3.5–4.9
Anal-fin base length	5.0	5.1–6.7
Pectoral-fin length	7.5	8.5–10.6
Pre-dorsal length	73.6	70.1–76.7
Pre-anal length	71.0	66.0–71.9
Head length	9.7	9.9–11.4
Percentage of head length		
Head depth	50.6	46.4–49.1
Head width	79.0	77.2–83.0
Preorbital length	33.7	36.4–43.9
Eye diameter	8.9	8.3–14.5
Interorbital width	28.9	25.6–35.1

Holotype. UFRJ 12667, 42.7 mm SL; Brazil: Estado do Rio de Janeiro: Município de Rio das Ostras: small stream inside União Biological Reserve, Rio Macaé basin, 22°26′10″ S 42°03′04″ W, about 20 m asl; LASEPT team, 9 November 2012.

Paratypes. UFRJ 9065, 1, 25.5 mm SL; UFRJ 9996, 1 (C&S), 26.5 mm SL; CICCAA 04081, 1, 31.7 mm SL; same collecting data as holotype. – UFRJ 9693, 1 (DNA), 32.5 mm SL; UFRJ 9758, 2 (C&S), 27.3–29.2 mm SL; same locality as holotype; A. M. Katz, M. A. Barbosa and F. R. Pereira, 6 September 2013.

Diagnosis. Listrura macaensis is distinguished from all other congeners of the subgenus *Listrura* by having weakly ossified antorbital and sesamoid supraorbital (Figure 4D; vs. well ossified, Figure 4C). *Listrura macaensis* also differs from *L. macacuensis* and *L. nematopteryx* by having a shorter extremity of the parurohyal lateral process, its distal core shorter than the proximal membranous region (Figure 4P; vs, longer, Figure 4O); from *L. costai* and *L. picinguabae* by having a different morphology of the anterior portion of the mesethmoid, in which there is a distinctive narrowing on the mesethmoidal region just posterior to the cornu, posteriorly followed by an abrupt widening (Figure 4D; vs. gradually widening); and from *L. picinguabae* by having a colour pattern consisting of dark pigmentation concentrated above the longitudinal midline of the flank (vs. dark blotches scattered above and below the lateral midline of the flank). *Listrura macaensis* is distinguished from an undescribed species from the Rio São João basin (*Listrura* sp. 2 in the analysis), supported in the analysis as its sister group (Figure 1), by the presence of a dorsal fin (vs. absence).

Description. Morphometric data appear in Table 1. Body slender, subcylindrical anteriorly, compressed posteriorly. Greatest body depth in area at mid-length between pectoral fin base and anal-fin origin. Dorsal profile of head and trunk approximately straight, slightly convex on caudal peduncle; ventral profile straight to slightly convex. Head trapezoidal in dorsal view. Anterior profile of snout about straight in dorsal view. Eye small, dorsally positioned in head, on its anterior half. Posterior nostril located slightly nearer orbital rim than anterior nostril. Tip of maxillary barbel reaching area between opercular patch of odontodes and pectoral-fin base; rictal and nasal barbels reaching posterior part of opercular patch of odontodes. Mouth subterminal. Jaw teeth slightly pointed, gently curved inside mouth, arranged in two rows; total premaxillary teeth 16–22, external row 6–11, internal row 10–13; total dentary teeth 14–18, external row 6 or 7, internal row 8–11. Branchial membrane attached to isthmus only at its anterior point. Branchiostegal rays 6.

Dorsal and anal fins small, with rounded distal margin; total dorsal-fin rays 7–9 (i–ii + III–VI + i), total anal-fin rays 7–8 (i + V–VI + i); dorsal-fin origin in vertical nearly

through anal-fin origin or slightly anterior to it; both dorsal-fin and anal-fin origin at vertical between 32nd and 34th vertebra centra. Pectoral fin filiform, with single, well-developed segmented unbranched ray. Pelvic fin and girdle absent. Caudal fin continuous to long skin folder sheltering procurrent rays, extending dorsally and ventrally to caudal peduncle, anteriorly contacting dorsal and anal fins, forming spatula-like tail, its largest depth slightly smaller than largest preanal depth; total principal caudal-fin rays 11–12 (I + 8 + II–III), total dorsal procurrent rays 29–31 (xxix–xxxi), total ventral procurrent rays 26–31 (xxvi–xxxi). Vertebrae 50–52. Ribs 3. Hypurals and parhypural fused, forming single plate, with minute anteromedian opening.

Latero-sensory system: supraorbital and infraorbital sensory canals absent; Postorbital canal with 2 pores: po1, in vertical line above dorsal process of opercle, and po2, in vertical line just posterior to opercular odontodes. Lateral line of body short, with 2 pores.

Osteology: anterior portion of mesethmoid T-shaped in dorsal view, anterior margin about straight to slightly concave; cornu rod-shaped, about straight to slightly curved; distinctive narrowing just posterior to cornu, posteriorly followed by abrupt widening at level of autopalatine middle portion. Lateral ethmoid with prominent lateral process just posterior to autopalatine body. Antorbital thin, slender; sesamoid supraorbital minute. Premaxilla sub-triangular in dorsal view, with sharply pointed lateral extremity; small process on posteromedial portion of dorsal surface, adjacent mesethmoid cornu base. Maxilla boomerang-shaped, slender, slightly shorter than maxilla. Autopalatine subtrapezoidal in dorsal view, broader anteriorly, postero-lateral process indistinct; flat narrow ossification, postero-medially directed, weakly dorsally inclined, attached to postero-lateral tip of autopalatine. Metapterygoid minute, oval. Quadrate slender, its dorsal process with broad posterior laminar process. Hyomandibula long, with sharply pointed anterior process. Opercle slender, with six or seven odontodes; odontodes pointed, nearly straight to slightly curved, arranged transversely; dorsal process of opercle triangular. Interopercle short, odontode patch length about twice opercular odontode patch depth, with seven odontodes; odontodes pointed, arranged in two irregular longitudinal rows; anterior margin of interopercle truncate; antero-dorsal process prominent. Preopercle long, its posterior tip reaching base of hyomandibula articular facet for opercle. Parurohyal slender, lateral process latero-posteriorly directed, long, sharply pointed, its distal core shorter than proximal membranous region; parurohyal head moderate, with small anterolateral paired process; middle foramen oval; posterior process rudimentary.

Colouration in alcohol: dorsum and dorsal portion of flank and head light yellowish grey, with superficial brown chromatophores, often forming small spots; dark brown to black stripe along flank longitudinal midline; broad unpigmented area below orbit. Venter and ventral portion of flank and head yellowish white, with brown chromatophores, more concentrated on posterior part of flank. Fins hyaline with minute dark brown chromatophores on basal portion of unpaired fin rays; vertically elongated dark brown spot on basal portion of caudal fin. Similarly coloured in life.

Distribution. Listrura macaensis is only known from the type locality, a stream inside the União Biological Reserve, Rio Macaé basin, south-eastern Brazil (Figure 2).

Etymology. The name *macaensis* is an allusion to the occurrence of the new species in the Rio Macaé basin.

Listrura macacuensis sp. nov.

LSID: urn:lsid:zoobank.org:act:A1BF567B-1C05-4726-B7F8-E8F9A25BE92F.
Figure 8; Table 2.

Figure 8. *Listrura macacuensis* sp. nov., UFRJ 12669, holotype, 29.8 mm SL.

Table 2. Morphometric data of *Listrura macacuensis* sp. nov.

	Holotype	Paratypes (n = 12)
Standard length (SL)	29.8	32.0–40.2
Percentage of standard length		
Body depth	8.7	7.7–9.8
Caudal peduncle depth	9.3	8.0–10.0
Body width	5.4	3.7–5.3
Caudal peduncle width	2.1	1.7–2.9
Dorsal-fin base length	3.5	3.1–4.1
Anal-fin base length	4.7	4.1–5.4
Pectoral-fin length	8.7	6.9–8.7
Pre-dorsal length	69.1	67.7–80.1
Pre-anal length	67.1	64.8–77.4
Head length	9.7	7.7–9.7
Percentage of head length		
Head depth	51.2	50.3–63.3
Head width	93.0	88.5–105.0
Pre-orbital length	36.5	25.3–41.9
Eye diameter	5.1	4.6–6.3
Interorbital width	22.2	22.2–30.7

Holotype. UFRJ 12669, 29.8 mm SL; Brazil: Estado do Rio de Janeiro: Município de Cachoeiras de Macacu: stream crossing the road Antônio José to Faraó, Rio Macacu basin, 22°31′02″ S 42°39′20″ W, about 45 m asl; A.M. Katz & P.J. Vilardo, 20 August 2019.

Paratypes. UFRJ 9268, 9, 12.0–19.6 mm SL; UFRJ 9279, 32, 16.5–41.8 mm SL, same locality as UFRJ 12669; UFRJ 9691, 3 (C&S), 26.7–38.7 mm SL; CICCAA 04081, 2, 31.0–31.4 mm SL; same locality as holotype; A.M. Katz, F.R. Pereira, C. Mello & O. Simões, 22 January 2013.

Diagnosis. Listrura macacuensis differs from all species of the subgenus *Listrura*, except *L. nematopteryx*, by having a long extremity of the parurohyal lateral process, with its distal core longer than the proximal membranous region (Figure 4O; vs., shorter, Figure 4P); it differs from *L. nematopteryx*, its sister species according to the analysis (Figure 1), by having dorsal-fin origin posterior to anal-fin origin (vs. anterior), more interopercular odontodes (8–10 vs. 5–7), and fewer vertebrae (49–50, vs. 51–52). *Listrura macacuensis* is also distinguished from *L. picinguabae* by having fewer vertebrae (49–50, vs. 52–55) and a colour pattern consisting of dark pigmentation concentrated above the longitudinal midline of the flank (vs. dark blotches scattered above and below the lateral midline of the flank); from *L. macaensis* by having well-ossified antorbital and sesamoid supraorbital (Figure 4C; vs. poorly ossified, Figure 4D); from *L. costai* and *L. picinguabae* by having a different morphology of the anterior portion of the mesethmoid, in which there is a distinctive narrowing on the mesethmoidal region just posterior to the cornu, posteriorly followed by an abrupt widening (Figure 4C; vs. gradually widening); and from *Listrura* sp. from the Rio São João basin by the presence of the dorsal fin (vs. absence).

Description. Morphometric data appear in Table 2. Body slender, subcylindrical anteriorly, compressed posteriorly. Greatest body depth in area at mid-length between

pectoral fin base and anal-fin origin. Dorsal profile of head and trunk approximately straight, slightly convex on caudal peduncle; ventral profile straight to slightly convex. Head trapezoidal in dorsal view. Anterior profile of snout about straight in dorsal view. Eye small, dorsally positioned in head, on its anterior half. Posterior nostril located slightly nearer orbital rim than anterior nostril. Tip of maxillary barbel reaching area between opercular patch of odontodes and pectoral-fin base; rictal and nasal barbels reaching posterior part of opercular patch of odontodes. Mouth subterminal. Jaw teeth slightly pointed, gently curved inside mouth, arranged in two rows; total premaxillary teeth 19–26, external row 6–9, internal row 13–17; total dentary teeth 17–19, external row 8 or 9, internal row 9 or 10. Branchial membrane attached to isthmus only at its anterior point. Branchiostegal rays 6.

Dorsal and anal fins small, with rounded distal margin; total dorsal-fin rays 6–8 (i + V–VII), total anal-fin rays 8–9 (ii + VI–VII); dorsal-fin origin posterior to anal-fin origin; first ray of both dorsal and anal fin at vertical between 32nd and 33rd vertebra centra. Pectoral fin filiform, with single, well-developed segmented unbranched ray. Pelvic fin and girdle absent. Caudal fin continuous to long skin folder sheltering procurrent rays, extending dorsally and ventrally to caudal peduncle, anteriorly contacting dorsal and anal fins, forming spatula-like tail, its largest depth slightly smaller than largest preanal depth; total principal caudal-fin rays 12 (I + 7–8 + III–IV), total dorsal procurrent rays 30–32 (xxx–xxxii), total ventral procurrent rays 28–29 (xxviii–xxix). Vertebrae 49–50. Ribs 3. Hypurals and parhypural fused, forming single plate, with minute anteromedian opening.

Latero-sensory system: supraorbital and infraorbital sensory canals absent; postorbital canal with 2 pores: po1, in vertical line above dorsal process of opercle, and po2, in vertical line just posterior to opercular odontodes. Lateral line of body short, with 2 pores.

Osteology: anterior portion of mesethmoid T-shaped in dorsal view, anterior margin about straight; cornu rod-shaped, about straight; distinctive narrowing just posterior to cornu, posteriorly followed by abrupt widening at level of limit between posterior margin of anterior autopalatine cartilage and anterior margin of osseous portion of autopalatine. Lateral ethmoid with prominent lateral process just posterior to autopalatine body. Antorbital well-developed, thin, drop-shaped; sesamoid supraorbital small, well-ossified. Premaxilla sub-triangular in dorsal view, with sharply pointed lateral extremity; small process on posteromedial portion of dorsal surface, adjacent mesethmoid cornu base. Maxilla boomerang-shaped, slender, about equal to maxilla. Autopalatine subtrapezoidal in dorsal view, broader anteriorly, postero-lateral process indistinct; flat narrow ossification, postero-medially directed, weakly dorsally inclined, attached to postero-lateral tip of autopalatine. Metapterygoid minute, oval. Quadrate slender, its dorsal process with broad posterior laminar process. Hyomandibula long, with sharply pointed anterior process. Opercle slender, with 6–8 odontodes; odontodes pointed, nearly straight to slightly curved, arranged transversely; dorsal process of opercle triangular. Interopercle short, odontode patch length about twice opercular odontode patch depth, with 10 or 11 odontodes; odontodes pointed, arranged in two irregular longitudinal rows; anterior margin of interopercle truncate; antero-dorsal process prominent. Preopercle long, its posterior tip reaching base of hyomandibula articular facet for opercle. Parurohyal slender, lateral process latero-posteriorly directed, long, sharply pointed, its distal core longer than proximal membranous region; parurohyal head small, with almost indistinct anterolateral paired process; middle foramen oval; posterior process rudimentary.

Colouration in alcohol: dorsum and dorsal portion of flank and head light yellowish grey, with superficial brown chromatophores; dark brown stripe along flank longitudinal midline; broad unpigmented area below orbit. Venter and ventral portion of flank and head greyish white, often with brown chromatophores longitudinally concentrated on posteroventral limit of flank. Fins hyaline with minute dark brown chromatophores on basal portion of unpaired fin rays. Similarly coloured in life.

Distribution. Listrura macacuensis is known from a single locality, a small stream of the Rio Macacu basin, south-eastern Brazil (Figure 2).

Etymology. The name *macacuensis* refers to the occurrence of the new species in the Rio Macacu basin.

Paralistrura, New Subgenus

LSID: urn:lsid:zoobank.org:act:33AEEE5C-E2A4-45FA-8D31-3E750A847084.

Type species. *Listrura tetraradiata* Landim & Costa, 2004.

Diagnosis. Paralistrura is distinguished from the subgenera *Listrura* and *Prolistrura* by the following apomorphic features: presence of a latero-dorsally directed process on the postero-medial margin of the autopalatine (chast.13.1, Figure 4B; vs. absence); and a long interopercular odontode patch, its length about twice larger than the opercular odontode patch (chast.24.1, Figure 4I; vs. about equal or smaller, Figure 4J). Also distinguished from both *Listrura* and *Prolistrura* by having a well-developed pectoral fin, with four rays (vs. a barbel-like pectoral fin, with a single ray in the subgenus *Listrura*, and a rudimentary pectoral fin, with a short first ray followed by one to three rudimentary rays), more teeth in the premaxilla (27–32 vs. 15–23) and dentary (24–31 vs. 13–21), dorsal and anal fins with branched rays (vs. all rays unbranched), and absence of ornamentation on the lateral margin of the lateral ethmoid; from *Listrura* by having fewer vertebrae (43–45 vs. 49–55), absence of a pronounced subcylindrical process on the lateral margin of the lateral ethmoid (vs. presence, Figure 4C,D), absence of a laminar extension on the posterior margin of the dorsal process of the quadrate (vs. presence, Figure 4A), caudal fin with 13 principal caudal-fin rays, of which ten are branched (vs. 11 or 12 principal caudal-fin rays, of which seven or eight are branched), and anal-fin origin posterior to dorsal-fin origin, in a vertical through dorsal-fin principal rays (vs. just anterior or just posterior to dorsal-fin origin, in a vertical anterior to dorsal-fin principal rays).

Included taxa. Only the type species, *L. tetraradiata*.

Distribution. Rio Ibicuíba drainage, Lagoa de Araruama basin, south-eastern Brazil (Figure 2).

Etymology. From the Greek *para* (a prefix meaning 'next to' or alternatively 'closely related') and *Listrura*, a genus of microcambevine trichomycterids, a name also derived from the Greek ('listros' meaning shovel, and 'ura' meaning tail), referring to its sister phylogenetic position to the subgenus *Listrura*. Gender feminine.

Prolistrura, New Subgenus

LSID: urn:lsid:zoobank.org:act:D9E0BDBC-1E01-4B4C-9361-AD8A9FF2791F.

Type species. *Listrura camposi* (Miranda Ribeiro, 1957).

Diagnosis. Prolistrura differs from the other subgenera of *Listrura* by the presence of a flattened, subtriangular projection on the lateral margin of the lateral ethmoid (chast.3.1., Figure 4A; vs. presence of pronounced process in *Listrura*, Figure 4C,D, and a minute flap in *Paralistrura*, Figure 4B), by having the dorsal and ventral hypurals plates in close proximity or united, but always keeping a longitudinal middle groove and a posterior gap (Figure 4H; vs. ankylosed, without a posterior gap, but often with an antero-middle notch, Figure 4K), and a small pectoral fin, with a well-developed first ray, followed by one or two rudimentary rays (chast.46.1; vs. a barbel-like single-rayed pectoral fin in *Listrura* and a broad pectoral fin with four well-developed rays). *Prolistrura* is also distinguished from *Listrura* by the absence of a laminar extension on the posterior margin of the dorsal process of the quadrate (vs. presence, Figure 4J), caudal fin with nine or ten branched rays (vs. seven or eight), and anal-fin origin posterior to the dorsal-fin origin, in a vertical through dorsal-fin principal rays (vs. just anterior or just posterior to dorsal-fin origin, in a vertical anterior to dorsal-fin principal rays); and from *Paralistrura* by the absence of a latero-dorsally directed process on the postero-medial margin of the autopalatine (vs. presence, Figure 4B) and a short interopercular odontode patch, its length about equal or smaller than the opercular odontode patch (vs. about twice larger), fewer teeth in the premaxilla (15–23 vs. 27–32) and dentary (13–21 vs. 24–31).

Included taxa. *Listrura boticarioi*, *L. camposi*, *L. depinnai* and one undescribed species included in the analysis. Other four apparently undescribed species are under study by the authors.

Distribution. Between Rio Ribeira de Iguape and Lagoa dos Patos basins, south-eastern and southern Brazil (Figure 2).

Etymology. From the Greek *pro* (a prefix meaning 'before', but also used in the sense of 'primitive') and *Listrura*, a genus of microcambevine trichomycterids, a name also derived from the Greek ('listros' meaning shovel, and 'ura' meaning tail), an allusion to its phylogenetic position as sister to a clade including the other two subgenera of *Listrura*. Gender feminine.

3.2.2. *Microcambeva* Costa & Bockmann, 1994

Microcambeva Costa & Bockmann, 1994: 718 (type species *Microcambeva barbata* Costa & Bockmann, 1994 by original designation and monotypy).

Diagnosis. *Microcambeva* is distinguished from *Listrura*, the only other genus of the Microcambevinae, by the following apomorphies: a long maxilla, distinctively longer than the premaxilla (chast.8.1–2., Figure 4E–H; vs. equal or slightly longer, Figure 4A–D), a broad opercular odontode patch, larger than cartilage articulating hyomandibula and neurocranium (chast.21.1, Figure 4K,L; vs. smaller, Figure 4I,J), the presence of a small process on the sub-proximal region of the ceratobranchial 4 (chast.32.1, Figure 4N; vs. absence, Figure 4M), and a bilobed caudal fin (chast.43.1, Figure 6E–G; vs. rounded, Figure 6A–D). *Microcambeva* is also distinguished from *Listrura* by the absence of a lateral widening in the mesethmoid, between anterior cornua and lateral ethmoid (vs. presence, Figure 4A–D), presence of a posterior process on the vomer (Figure 5E; vs. absence), presence of a well-developed postero-lateral process on the autopalatine (Figure 4E–H; vs. rudimentary, Figure 4A–D), absence of a narrow and flat ossification, postero-medially directed, on the postero-medial margin of the autopalatine (vs. presence, Figure 4A–D), a rod-shaped antorbital (Figure 4E–H; vs. comma-shaped, Figure 4A–D), a well-developed sesamoid supraorbital (Figure 4E–H; vs. rudimentary, Figure 4A–D), the presence of the median segment of the supraorbital latero-sensory canal, corresponding to the segment between pores s4 and s6 (Figure 5B,C; vs. absence), the absence of a constriction on the interopercle, above odontode patch (vs. presence, Figure 4I,J), presence of a cranial fontanel (Figure 4I,J; vs. absence), a well-ossified hypobranchial 3 (Figure 4N; vs. weakly or not ossified, Figure 4M), a fusiform trunk (Figure 6E–G; vs. ell-like, Figure 6A–D), absence of an anterior process on the neural spines of precaudal vertebrae (vs. presence, Figure 5F), procurrent caudal-fin rays restricted to area adjacent to the caudal fin (vs. anteriorly extending to an area close to the dorsal and anal fins), dorsal and hypural plates separated by broad interspace (Figure 5I,J; vs. in close proximity, partially or completely ankylosed, Figure 5H,K), pelvic fin present (vs. absent); trunk transparent, with a few minute patches of chromatophores (Figure 6E–G; vs. well pigmented, Figure 6A–D), fewer procurrent caudal-fin rays (5–8 on the dorsal, 5–9 on the ventral part, vs. 21–39 and 21–36, respectively), and fewer vertebrae (33–36 vs. 43–55).

Included taxa. Eight species in three subgenera, as below listed (Figure 3). The species *Pygidium triguttatum* Eigenmann, 1918, known only from its type series containing five specimens collected in Jacareí, Rio Paraíba do Sul basin, south-eastern Brazil, by John Haseman in 1908, possibly belongs to *Microcambeva*. Photographs and radiographs of the holotype deposited in the Field Museum of Natural History (FMNH 58670, 30.6 mm SL; https://collections-zoology.fieldmuseum.org/catalogue/637990, accessed on 9 November 2021) indicates that it is a member of the TSVSGM-clade by having the following derived features: absence of the infraorbital sections of the cephalic latero-sensory system, presence of a slender parurohyal, with a narrow and elongate lateral process, and only a total of three ribs. The presence of a sinuous anterior margin of the autopalatine osseous portion supports its inclusion in the Microcambevinae. The following apomorphies would support its inclusion in *Microcambeva*: the presence of a hypertrophied opercular odontode

patch, contrasting with a short interopercular odontode patch, minute chromatophores scattered on the body, and a long maxilla, about once and half longer than the premaxilla. However, it is not possible to see the presence of a small process on the sub-proximal region of the ceratobranchial 4, as well as the caudal fin is broken, not allowing to see the bilobed morphology. *Pygidium triguttatum* is superficially similar to *M. filamentosa*, the only species of *Trichocambeva* (see below) by having a long pectoral-fin filament and long barbels, besides having a concavity on the dorsal margin of the opercle and a similar autopalatine morphology, but it is not possible to check in available radiographs all the apomorphic conditions here listed for *Trichocambeva*. On the other hand, in *P. triguttatum* the cephalic latero-sensory system includes a well-developed canal with a paired supraorbital S6 pore, thus not exhibiting the apomorphic single S6 pore shared by *Pterocambeva* and *Trichocambeva*. Therefore, presently it is not possible to unambiguously assign *P. triguttatum* to any microcambevine taxon, although probably belonging to the genus *Microcambeva*.

Subgenus *Microcambeva*

Diagnosis. The subgenus *Microcambeva* is distinguished from the other subgenera by the following apomorphic features: the presence of a distinctive sharp, edentulous lateral process in the maxilla (chast.7.1, Figure 4F,G; vs. maxilla laterally terminating in a narrow tip, but without an edentulous process, Figure 4E,H) and the presence of an ossification on the anterior surface of the anterior cartilage head of the autopalatine (chast.14.1, Figure 4F,G; vs. absence). *Microcambeva* also differs from *Pterocambeva* and *Trichocambeva* by having: supraorbital pore s6 paired (vs. single), seven pectoral-fin rays (eight in *Pterocambeva* and six in *Trichocambeva*), and nasal barbel moderate in length, its tip posteriorly reaching orbit (vs. minute, barely reaching posterior nostril in *Pterocambeva* and long, reaching between opercular odontode patch and pectoral-fin base in *Trichocambeva*); from *Pterocambeva* by having a short posterior portion of the autopalatine, occupying about half two autopalatine length (Figure 4F,G; vs. long, about two thirds of the autopalatine length, Figure 4E) and a gradual and slight constriction in the anterior portion of the neurocranium (Figure 5C; vs. abrupt and strong, Figure 5B); and from *Trichocambeva* by the absence of a prominent expansion in the hyomandibula just anterior to the on the articulatory cartilage for the neurocranium (vs. presence, Figure 4L), the absence of a predorsal adipose fold (vs. presence), and the presence of a posterior extension in the ventral margin of the caudal fin, making it slightly asymmetrical in lateral view (Figure 6F; vs. symmetrical, Figure 6E). *Microcambeva* also differs from other microcambevines by the absence a flat ossification on the antero-lateral part of the ventral surface of the autopalatine, below the anterior cartilage; this ossification is present both in *Pterocambeva* and *Trichocambeva* (Figure 4E,H) and seems to be homologous to the more laterally placed ossification present in *Listrura* (Figure 4A), probably constituting an additional synapomorphic condition for Microcambevinae, with a structure loss in the subgenus *Microcambeva*.

Included taxa. Five species: *M. barbata*, *M. draco*, *M. jucuensis*, *M. mucuriensis*, and *M. watu*.

Distribution. Between Rio Jucuruçu and Rio São João basins, eastern and south-eastern Brazil (Figure 3).

Pterocambeva, New Subgenus

LSID: urn:lsid:zoobank.org:act:4563C29F-C031-4EC4-92B8-1A7C0988D533.

Type species. *Microcambeva ribeirae* Costa, Lima & Bizerril, 2004.

Diagnosis. Pterocambeva is distinguished from the subgenera *Microcambeva* and *Trichocambeva* by the following apomorphies: a long posterior portion of the autopalatine, occupying about two thirds of the autopalatine length (chast.10.1, Figure 4E; vs. short, about half length or slightly less, Figure 4F–H), an abrupt and strong constriction in the anterior portion of the neurocranium (chast.27.1, Figure 5B; vs. slight constriction, Figure 5C), a robust pectoral fin, with the first pectoral-fin ray shorter than adjacent rays (chast.47.1, Figure 9D; vs. thin and longer than adjacent rays, Figure 9B) and a hypertrophied major proximal radial (Figure 5M; vs. not hypertrophied, Figure 5N,O), and a minute nasal barbel,

barely reaching posterior nostril (chast.54.1, Figure 9C; vs. longer, reaching eye or posterior to it, Figure 9A). Also distinguished from *Microcambeva* by the absence of a distinctive lateral process in the maxilla (vs. presence, Figure 4F,G), by having eight pectoral fin rays (vs. seven), and by the absence of an ossification on the anterior surface of the anterior cartilage head of the autopalatine (vs. presence, Figure 4F,G); and from *Trichocambeva* by the absence of a prominent expansion in the hyomandibula just anterior to the articulatory cartilage for the neurocranium (vs. presence, Figure 4L), the absence of a hypertrophied predorsal adipose fold (vs. presence, Figure 6E), a posteriorly expanded ventral lobe of the caudal fin, making it slightly asymmetrical in lateral view (Figure 6F; vs. not expanded, Figure 6E), and eight pectoral-fin rays (vs. six).

Figure 9. Head and anterior portion of trunk: (**A**,**C**), left lateral view, (**B**,**D**) dorsal view, of: (**A**,**B**) *Microcambeva* (*Trichocambeva*) *filamentosa*, UFRJ 12187, 31.4 mm SL, (**C**,**D**) *Microcambeva* (*Pterocambeva*) *ribeirae*, UFRJ 12189, 33.3 mm SL. Modified from (17): Figure 3. The numbers are characters, followed by character states after dots, which are numbered according to Appendix C.

Included taxa. Two species, *M. bendengo* and *M. ribeirae*.

Distribution. Rio Macacu and Rio Ribeira de Iguape basins, south-eastern Brazilian coastal plains (Figure 3).

Etymology. From the Greek *ptero* (wing) and *cambeva*, a popular name for trichomycterids in south-eastern and southern Brazil and a nominal trichomycterine genus, referring to the broad and slightly curved margin, remembering a bird wing, with irregular posterior margin due to deep gaps on the fin membrane, resembling feathers. Gender feminine.

Trichocambeva, New Subgenus

LSID: urn:lsid:zoobank.org:act:3B20988A-FF87-4480-A199-E19DA49D93C2.

Type species. *Microcambeva filamentosa* Costa, Katz & Vilardo, 2020.

Diagnosis. Trichocambeva is distinguished from *Pterocambeva* and *Microcambeva* by the following apomorphic features: presence of a prominent expansion in the hyomandibula just anterior to the articulatory cartilage for the neurocranium (chast.19.1, Figure 4L; vs. absence), the presence of a predorsal adipose fold (chast.39.1, Figure 6E; vs. absence), first pectoral-fin ray terminating in long filament, about 70–80% of the pectoral-fin length without the filament (chast.48.1, Figure 9B; vs. filament when present minute, 20% or less of that length), and a long nasal barbel, reaching between the opercular odontode patch and the pectoral-fin base (chast.54.2, Figure 6A; vs. reaching orbit or anterior to it). Also distinguished from *Pterocambeva* and *Microcambeva* by: dorsal and ventral lobe of the caudal fin equal in length (Figure 6E; vs. ventral lobe longer, Figure presence of an extension, making the caudal fin slightly asymmetrical), absence of a paired barbel-like structure on the branchiostegal region (vs. presence, Figure 9C), and six pectoral-fin rays (vs. seven or eight); from *Pterocambeva* by having a shorter posterior portion of the autopalatine, occupying about half two autopalatine length (Figure 4H; vs. long, about two thirds of the autopalatine length, Figure 4E) and the absence of an abrupt and strong constriction in the anterior portion of the neurocranium (vs. presence, Figure 5B); and from *Microcambeva* by the absence of a distinctive edentulous lateral process in the maxilla (vs. presence, Figure 4F,G) and absence of an ossification on the anterior surface of the anterior cartilage head of the autopalatine (vs. presence, Figure 4F,G).

Included taxa. Only the type species, *M. filamentosa*.

Distribution. Rio Ribeira de Iguape basin, south-eastern Brazil (Figure 3).

Etymology. From the Greek *trichos* (hair or hair-like) and *cambeva*, a popular name for trichomycterids in south-eastern and southern Brazil and a nominal trichomycterine genus, an allusion to the long barbels and long pectoral-fin filament. Gender feminine.

3.3. Key for Identification of Genera and Subgenera of Microcambeviinae

A1. Trunk ell-like, opaque in life, widely pigmented; pelvic fin absent; caudal fin rounded, procurrent caudal-fin rays anteriorly extending to an area close to the dorsal and anal fins . . . . . B (genus *Listrura*)

A2. Trunk fusiform, transparent in life, with a few minute patches of chromatophores; pelvic fin present; caudal fin bilobed, procurrent caudal-fin rays restricted to area adjacent to the caudal fin . . . . . D (genus *Microcambeva*)

B1. Pectoral fin narrow, with three or fewer rays; all dorsal and anal fin rays unbranched C

B2. Pectoral fin broad, with four rays; posterior dorsal and anal fin rays branched . . . . . subgenus *Paralistrura*

C1. Pectoral fin barbel-like, with single ray; caudal fin with seven or eight branched rays; anal-fin origin just anterior or just posterior to the dorsal-fin origin, in a vertical anterior to dorsal-fin principal rays . . . . . subgenus *Listrura*

C2. Pectoral fin with a short first ray, followed by one or two rudimentary rays; caudal fin with nine or ten branched rays; anal-fin origin posterior to the dorsal-fin origin, in a vertical through dorsal-fin principal rays . . . . . subgenus *Prolistrura*

D1. First pectoral-fin ray never with a long filament; pectoral-fin rays seven or eight; ventral procurrent-caudal fin rays four to seven; a short or minute nasal barbel, reaching orbit or anterior to it; presence of a paired barbel-like structure on the branchiostegal region; with a posterior extension in the ventral margin of the caudal fin, making it slightly asymmetrical; without a hypertrophied predorsal adipose fold . . . . . E

D2. First pectoral-fin ray terminating in long filament, about 70–80% of the pectoral-fin length without the filament; pectoral-fin rays six; ventral procurrent-caudal fin rays nine; a long nasal barbel, reaching between the opercular odontode patch and the pectoral-fin base; absence of a paired barbel-like structure on the branchiostegal region; without a posterior extension in the ventral margin of the caudal fin; with a predorsal adipose fold . . . . . subgenus *Trichocambeva*

E1. Supraorbital pore s6 single; first pectoral-fin ray robust and shorter than adjacent rays; eight pectoral-fin rays; nasal barbel minute, barely reaching posterior nostril . . . . . subgenus *Pterocambeva*

E2. Supraorbital pore s6 paired; first pectoral-fin ray thin and longer than adjacent rays, terminating in short filament; seven pectoral-fin rays; nasal barbel moderate in length, reaching orbit . . . . . subgenus *Microcambeva*

4. Discussion

4.1. Phylogenetic Relationships and Morphological Support

In addition to the two morphological character states described by Costa et al. [3] supporting monophyly of Microcambevinae, the present analysis indicated the presence of a sinuous anterior margin of the osseous portion of the autopalatine (Figure 4A–D,F–H) as a synapomorphy for this subfamily (Figure 1). However, according to the analysis, this apomorphic condition is reversed in *Pterocambeva*, in which the general morphology of the autopalatine is modified to acquire an elongated morphology (Figure 4E). Another derived condition occurring in the same region of the autopalatine of microcambevines, possibly related to that condition above described, is the presence of a flat ossification attached to the anteroventral portion of the autopalatine, placed close or at the lateral bone margin. In the genus *Listrura*, the ossification is placed laterally to the anterior cartilage (Figure 4A), whereas in the subgenera *Pterocambeva* and *Trichocambeva* it runs ventrally to it (Figure 4E,H), but in *Microcambeva* this ossification is absent. Developmental studies are necessary to check if the flat autopalatine ossifications in the genera *Listrura* and *Microcambeva* in fact correspond to homologous conditions.

The present phylogenetic analysis supported sister group relationships between *Pterocambeva* and *Trichocambeva*, thus providing a result identical to that obtained when molecular data were analysed alone [3]. However, only two morphological character states support monophyly of the clade containing only *Pterocambeva* and *Trichocambeva*: the presence of a single supraorbital s6 pore and a concavity on the dorsal margin of the opercle (Figure 4K,L). This morphological evidence supporting the clade is substantially weaker than that supporting a supposed clade comprising the subgenera *Microcambeva* and *Pterocambeva*, including the following apomorphic conditions: eyes large and posteriorly placed on head (Figure 6F,G), presence of a paired barbel-like structure on the branchiostegal region (Figure 9C), a long maxilla that is about twice or more the premaxilla length, excluding the lateral process (Figure 4E–G), a long, anteriorly broadened ventral hypural plate, yielding a sub-rectangular morphology (Figure 5I), and an ossified minor proximal radial of the pectoral fin (Figure 5M,N). Based on the hypothesis depicted in the tree topology here supported (Figure 1), these derived features may be interpreted either as a result of convergent traits occurring in the diurnal taxa *Microcambeva* and *Pterocambeva*, or basal conditions for the genus *Microcambeva* with reversals in the putative nocturnal *Trichocambeva* (see discussion below).

4.2. Morphological Diversity and Evolution of Fossorial Lifestyle in Listrura

Species having fossorial habits are certainly among the lesser known among teleost fishes, often being discovered by chance encounters [39]. For example, species of the West African synbranchid genus *Typhlosynbranchus* Pellegrin, 1922 are only known from a few specimens, with part of them accidentally found during caecilian amphibian collections [40]. Similarly, the Amazon characiform *Tarumania walkerae* de Pinna, Zuanon, Py-Daniel & Petry, 2017, the only representative of the Tarumanidae, was first found deeply buried in leaf-litter forest swamps during a limnological survey [41]. Besides being rare or living in habitats hardly accessible to common fish collectors, fossorial teleosts tend to share some morphological traits, such as an elongate eel-shaped body with numerous vertebrae and reduction or loss of fins [3,42,43]. For this reason, species of the genus *Listrura* are typical fossorial fishes by living burrowed in leaf-litter or muddy substratum, having elongated eel-shaped body with numerous vertebrae, and fins reduced or absent, conditions that are homoplastically found in glanapterygines (see results above). Due to the shared possession of such convergent character states, *Listrura* was formerly included in the Glanapteryginae (see Costa et al. [3] for a historical review on the subfamilies Glanapteryginae and Sarcoglanidinae). The present study once again supports the convergent acquisition of these three features in the Amazon fossorial glanapterygine *P. amphioxus* (Figure 1).

Typical morphological adaptations for fossorial lifestyle may arise independently (i.e., parallel evolution) in different lineages of a single interstitial teleost fish group. For example, molecular data support repeated evolution of convergent morphotypes in the Mediterranean clingfish genus *Gouania* Nardo, 1833, with different species independently acquiring more elongated body with more vertebrae [44]. Similarly, the present analysis supports dorsal fin loss as independently occurring in the subgenera *Listrura* (i.e., *Listrura* sp. 2) and *Prolistrura* (i.e., *L. depinnai*; Figure 1). Another species lacking dorsal fin, *L. boticario*, described based on a single specimen [9] and not included in the present analysis (see materials and methods above), is a typical member of *Prolistrura*, like *L. depinnai*. However, its colour pattern [45] that is nearly identical to that described for *L. camposi* [46] suggests close relationships with this species inhabiting the same geographical area (Figure 2), not with *L. depinnai*, the other species of *Prolistrura* lacking dorsal fin. If so, the dorsal fin would have been independently lost thrice in *Listrura*.

There is a great morphological gap between *L. tetraradiata*, the only species of *Paralistrura*, and its sister group, a clade comprising all species of the subgenus *Listrura*. The morphological gap is possibly resulting from a more specialised level of morphological adaptations for the fossorial lifestyle in the latter subgenus, since included species share a series of apomorphies typical of specialised fossorial species. Most informative characters to illustrate the morphological gap between these sister subgenera include the presence of a well-developed pectoral fin, with a total of four rays in *Paralistrura*, vs. a barbel-like pectoral fin with a single long ray in *Listrura*, and 43–45 free vertebrae in *Paralistrura*, vs. 49–55 in *Listrura*, besides species of the subgenus *Listrura* having a more slender body and caudal fin (compare Figure 6C,D). Considering the different kinds of habitat where species of these lineages were found (i.e., the species of *Paralistrura* associated to leaf litter deposits, about 40 cm deep, close to a stream margin, vs. species of *Listrura* deeply burrowed in leaf litter and mud, about 5 cm deep or less, in swampy areas covered by amphibious plants, peripheral to small streams [47]), the apomorphic morphological features exhibited by species of the subgenus *Listrura* probably are related to the more extreme habitat recorded for them. Among species of the subgenus *Listrura*, the most specialised species seems to be *L. picinguabae*, with more vertebrae (52–55 vs. 49–52) and shorter dorsal and anal fins [7].

Among species of *Prolistrura*, *L. depinnai* has a relatively deeper body (Figure 6A) and fewer vertebrae (45–46) than other congeners of the subgenus *Prolistrura*, which could be interpreted as plesiomorphic [11] or unspecialised conditions for fossorial lifestyle. However, these conditions probably are not plesiomorphic considering its phylogenetic position as sister to *Listrura* sp. 1, a slender species with more vertebrae (48–50), conditions that are similar to that observed in *L. camposi*, the sister group of the remaining species

of *Prolistrura* (Figure 1). In fact, the general morphology of *L. depinnai* may be related to a different habitat specialisation, since in its type locality it was found in a very shallow swamp, less than 1 cm between water surface and bottom, which comprised a dense layer of sphagnum, mud and leaf litter [11] (WJEMC personal observation, 25 September 2014), thus contrasting with the typical habitat of other congeners of *Prolistrura* (i.e., shallow pool, about 10 cm deep, associated to small streams, with leaf litter and sand on the bottom [46]). On the other hand, specimens of another population of *L. depinnai* were found in a habitat similar to those above reported fro other species of *Prolistrura* (AMK personal observation, 16 October 2019). These data suggest that *L. depinnai* would be possible to colonise different habitats. The unique general body morphology of *L. depinnai*, consisting of a more compact and compressed body, with a deep caudal peduncle as consequence of long procurrent caudal-fin rays (Figure 6A), highly resembles the general morphology of freshwater lungfishes, which are also fossorial species [48].

4.3. Morphological Diversity and Evolution of Psammophily in Microcambeva

Psammophily is a widespread lifestyle among trichomycterids, probably constituting the plesiomorphic condition for the TSVSGM-clade, besides convergently occurring in several other Neotropical teleost groups. For example, species belonging to different teleost fish groups have been reported to live in multispecies assemblages associated to the same sandy substratum, as reported by Zuanon et al. [49] when studying a sand-dwelling fish assemblage from central Amazonia. These authors noted some convergent morphological traits in psammophilic teleosts that are relevant for searching evolutionary aspects of psammophily in microcambevines and other trichomycterids: an acuminate snout, large and dorsally placed eyes, a small body size, and light coloured and/or translucent bodies (i.e., cryptic colour on sandy substratum). The presence of an acuminate snout, considered to be related with burying habits in the sand [50], involves different morphological structures in psammophilic members of each fish family [49]. The condition herein reported to be responsible for this snout morphology in microcambevines is the presence of a strong lateral compression on the antero-frontal portion of the neurocranium (Figure 5B), present in species of *Pterocambeva*, but homoplastically occurring in other two psammophilic trichomycterid genera, the sarcoglanidine *Stauroglanis* de Pinna, 1989 and the trichomycterine *Scleronema* Eigenmann, 1917 (Figure 1).

Other apomorphic conditions involving snout and adjacent structures herein supported as independently acquired in psammophilic microcambevines and other psammophilic trichomycterids are the presence of a long maxillary bone and an ossification on the anterior portion of the autopalatine cartilage. The presence of a relatively long maxilla has been reported to independently occur in different psammophilic trichomycterid lineages [3,18,20]. However, in all species of the genus *Microcambeva*, except in *M. filamentosa*, subgenus *Trichocambeva*, the maxilla is a distinctively long bone, with its length about twice or slightly more than the premaxilla length (Figure 4E–G), internally supporting the broad maxillary barbel base (Figure 6C), which is a highly specialized condition, independently occurring in some sarcoglanidines [3,51], including *S. gouldingi* here analysed (Figure 1). Curiously, species of the subgenus *Microcambeva* have a small ossification on the anterior portion of the autopalatine cartilage (Figure 4F,G), a neomorphic structure similar to that independently occurring in psammophilic sarcoglanidines [3,51,52], probably acting as an additional support for moving the long maxillary bone inside the robust maxillary barbel. Among species of *Microcambeva*, the ossification is considerably larger in *M. barbata*, in which the maxilla is conspicuously longer than in other species of the subgenus (compare Figure 4F,G). Equally remarkable is the presence of a paired barbel-like structure on the branchiostegal region of most species of *Microcambeva* (Figure 9C), but also reported to occur in the Amazon psammophilic sarcoglanidine *Malacoglanis gelatinosus* Weitzman & Myers, 1966 [53].

Zuanon et al. [49] reported multiple occurrences of small body size and light coloured or translucent bodies among psammophilic fish species, which were considered as paedomorphic

features. However, both small size and translucent body (Figure 6E–G), often with minute patches of multicolour chromatophores (e.g., Costa & Bockmann, 1994), are widespread conditions among members of different lineages of the TSVSGM-clade [5,52,54,55], probably constituting plesiomorphic conditions for the clade. Furthermore, Zuanon et al. [49] also reported the common occurrence of large and dorsally placed eyes in psammophilic teleosts, associated to visual orientation in the foraging behaviour of taxa such as *S. gouldingi*, a diurnal species that poises on the substrate supported by its pectoral fin [50], a behaviour similar to that reported for *M. ribeirae* [12] of the subgenus *Pterocambeva*. In *Pterocambeva*, the pectoral fin is robust, its external margin is slightly curved, and the first ray is conspicuously shorter than other rays (Figure 9D), like independently occurring in the psammophilic genus *Scleronema* (Figure 1). Another component of the apomorphic pectoral-fin morphology of *Pterocambeva* is the uniquely hypertrophied major proximal radial (Figure 5M).

Large, posteriorly placed eyes (Figure 6F,G), occur in all species of the genus *Microcambeva*, except *M. filamentosa* (Figure 6E). The possession of a small eye, long barbels, and long pectoral-fin filament (Figure 9A,B) in *M. filamentosa*, the only member of the subgenus *Trichocambeva*, contrasts with the large eye, short barbels and absence of pectoral-fin filament in species of the sister group, subgenus *Pterocambeva* (Figure 9C,D). The presence of these contrasting features in sister lineages was attributed to them evolutionarily diverging to use different strategies to exploit their habitat [16], with the former lineage exhibiting morphological characters of species predominantly using chemosensory and tactile detection of food (i.e., nocturnal habits), and the later with morphological characteristics typical of diurnal species using visual detection of food, like that described for *S. gouldingi* [50]. However, the present phylogenetic tree topology does not make clear if the large eye occurring in the subgenus *Microcambeva* (Figure 6G) has arisen independently from the large eye in *Pterocambeva*, or if the larger eye had its origin in the most recent common ancestor of the genus *Microcambeva*, with a reversal to smaller eyes in *Trichocambeva*. On the other hand, the very short nasal barbel in *Pterocambeva* is unambiguously supported as an apomorphic condition convergently acquired in the psammophilic *S. gouldingi* (Figure 1). Finally, the predorsal adipose fold, unique for *Trichocambeva* among microcambevines (Figure 6E), is similar to the dorsal fold described for specialised psammophilic glanapterygines with rudimentary or absent eyes, living deeply buried in the sand [56], thus suggesting that the morphological pattern exhibited by *Trichocambeva*, unique among congeners, consists of an adaptation for living more deeply buried into the sand. However, additional field studies are necessary to test this hypothesis.

5. Conclusions

The use of molecular tools in recent decades has significatively and rapidly improved our understanding of the phylogeny of teleost fishes, in some cases consistently supporting relationships not imagined before, when using only morphological data to infer relationships. For example, well corroborated molecular phylogenies [57,58] have shown that our previous classifications of major lineages of teleost fishes were mostly based on artificial (i.e., non-monophyletic) groups. In the specific case of the fish order herein studied, the Siluriformes (catfishes), an inclusive morphological phylogeny [59] supported a series of clades with transoceanic distribution (e.g., the African Amphiliidae plus Neotropical loricarioids; part of the South American Pimelodidae plus part of the Afro-Asiatic Bagridae; the South American Auchenipteridae and Doradidae plus the African Mochokidae; and the South American Aspredinidae plus the Asiatic families Amblycipitidae, Akisidae, Sisoridae, Erethistidae), all of them refuted by a well corroborated molecular phylogeny [60], showing that the available morphological phylogeny was greatly biased by superficially similar convergent character states. However, the present study shows that molecular and morphological data when combined may yield well-supported phylogenies, with a rich diversity of morphological characters useful to unambiguously diagnose clades and to establish hypothesis on morphological evolution.

Author Contributions: Conceptualization, W.J.E.M.C.; data obtaining, W.J.E.M.C. and A.M.K.; formal analysis, W.J.E.M.C.; investigation, W.J.E.M.C. and A.M.K.; data curation, W.J.E.M.C. and A.M.K.; writing—original draft preparation, W.J.E.M.C.; visualization, W.J.E.M.C. and A.M.K.; supervision, W.J.E.M.C.; project administration, W.J.E.M.C.; funding acquisition, W.J.E.M.C. and A.M.K. All authors have read and agreed to the published version of the manuscript.

Funding: This study was supported by Conselho Nacional de Desenvolvimento Científico e Tecnológico (CNPq; grant 304755/2020-6 to WJEMC), and Fundação Carlos Chagas Filho de Amparo à Pesquisa do Estado do Rio de Janeiro (FAPERJ; grant E-26/202.005/2020 to AMK and E-26/202.954/2017 to WJEMC). This study was also supported by CAPES (Coordenação de Aperfeiçoamento de Pessoal de Nível Superior, Finance Code 001) through Programa de Pós-Graduação em: Biodiversidade e Biologia Evolutiva /UFRJ; Genética/UFRJ; and Zoologia, Museu Nacional/UFRJ.

Data Availability Statement: DNA sequences used in this study are deposited in GenBank.

Acknowledgments: Thanks are due to P.F. Amorim, M.A. Barbosa, J.L. Mattos, C. Mello, F. R. Pereira, O. Simões, and P. Vilardo for help during collecting trips. Thanks to the Willi Hennig Society for making TNT available.

Conflicts of Interest: The author declares no conflict of interest.

Appendix A

Complete list of material of Microcambevinae examined (H, holotype; P, paratypes; C&S, specimens cleared and stained for bone and cartilage). Institutions: CICCAA, Centre of Agrarian and Environmental Sciences, Federal University of Maranhão, Chapadinha; MCP, Museu de Cências e Tecnologia, Universidade Pontifícia do Rio Grande do Sul, Porto Alegre; MNRJ, Museu Nacional, Rio de Janeiro; MZUSP, Museu de Zoologia, Universidade de São Paulo, São Paulo; UFRJ, Institute of Biology, Federal University of Rio de Janeiro, Rio de Janeiro.

***Listrura camposi*:** UFRJ 11404, 5 (2 C&S).
***Listrura costai*:** MNRJ 31917, H; MNRJ 31535, 3 P; MNRJ 31918, 5 P; MNRJ 39620, 4 P; UFRJ 7214, 3 P; UFRJ 6577, 3 P; UFRJ 7215, 4; UFRJ 7214, 6; UFRJ 11224, 4.
***Listrura depinnai*:** UFRJ 12552, 5; UFRJ 10689, 2 (1 C&S).
***Listrura nematopteryx*:** UFRJ 707, 20; UFRJ 8623, 1; UFRJ 5952, 5 (C&S).
***Listrura picinguabae*:** UFRJ 6111, H; MCP 38921, 2 P; UFRJ 5948, 1 P; UFRJ 5949, 2 P; UFRJ 5950, 15 P; UFRJ 5951, 4 P (C&S); UFRJ 5991, 2 P; UFRJ 6138, 5 P (C&S).
***Listrura tetraradiata*:** MZUSP 52572, H; UFRJ 4586, 17P; UFRJ 4588, 6 P (C&S); UFRJ 4587, 17 P; UFRJ 4590, 7 P; MZUSP 50164, 3 P; UFRJ 11458, 8; UFRJ 11457, 9.
***Listrura* sp. 1:** UFRJ 9601, 11; UFRJ 1278, 1; UFRJ 9692, 3 (C&S); UFRJ 11522, 2 (C&S); UFRJ 9498, 11; UFRJ 1279, 1 (C&S); UFRJ 9994, 1 (C&S).
***Microcambeva barbata*:** MZUSP 43678, H; MZUSP 43679, 1 P; UFRJ 684, 2 P (C&S); UFRJ 12129, 1; UFRJ 7000, 1 (C&S).
***Microcambeva draco*:** MCP 17796, H; MCP 17796, 1P (C&S).
***Microcambeva filamentosa*:** UFRJ 12187, P; UFRJ 12180, 2 P; UFRJ 12188, 1 P; UFRJ 12345, 2 P (C&S); UFRJ 12551, 9 P.
Microcambeva jucuensis: UFRJ 12124, H; UFRJ 11083, 18 P; UFRJ 11011, 4 P; UFRJ 11840, 4 P (C&S); CICCAA 03524, 2 P.
***Microcambeva mucuriensis*:** UFRJ 12123, H; UFRJ 11091, 22 P; UFRJ 11028, 4 P; UFRJ 11841, 5P (C&S); CICCAA 03525, 2 P;
***Microcambeva ribeirae*:** MZUSP 84301, H; MZUSP 78617, 5 P; MZUSP 68169, 3 P (C&S); MZUSP 74669, 10 P; MZUSP 79953, 20 P; MNRJ 12314, 1 P; MNRJ 14304, 4 P (1 C&S); MZUSP 49463, 1 P (C&S); UFRJ 12189, 2; UFRJ 6999, 1 (C&S); UFRJ 12549, 3.

Appendix B

Terminal taxa and respective GenBank accession numbers.

	COI	CYTB	RAG2
Trichogenes longipinnis	MK123682	MK123704	MF431117
Trichomycterus nigricans	MN813005	MK123723	MK123765
Ituglanis boitata	MK123684	MK123706	MK123758
Scleronema minutum	MK123685	MK123707	MK123759
Stauroglanis gouldingi	MN385800	KY858033	———-
Pygidianops amphioxus	MN385801	———-	MN385823
Homodiateus anistisi	MN385798	———-	MN385821
Microcambeva filamentosa	MN385808	OK334289	MN385831
Microcambeva ribeirae	MN385807	OK334290	MN385832
Microcambeva barbata	MN385804	———-	MN385829
Microcambeva jucuensis	MN385805	———-	MN385830
Microcambeva mucuriensis	MN385806	———-	MN385828
Listrura tetraradiata	JQ231083	JQ231088	MN385826
Listrura nematopteryx	HM245417	HM245425	———-
Listrura macacuensis	MN385802	OK143231	MN385825
Listrura macaensis	OK144133	OK143232	———-
Listrura costai	HM245414	HM245421	———-
Listrura picinguabae	HM245416	HM245424	———-
Listrura camposi	MK123703	MK123732	MN385824
Listrura depinnai	———-	OK143234	———-
Listrura sp. 1	MN385803	OK143233	MN385827
Listrura sp. 2	JN830897	JN830896	———-

Appendix C

List of morphological characters

1. Mesethmoid, main axis, area posterior to cornu basis, abrupt lateral widening: (0) absent; (1) present.
2. Mesethmoid, cornu, shape: (0) narrow and cylindrical; (1) broad and flat.
3. Lateral ethmoid, lateral margin, surface; (0) smooth, without projections; (1) with flattened, subtriangular projection; (2) with pronounced subcylindrical process.
4. Vomer, lateral constriction: (0) absent; (1) present.
5. Vomer, posterior process: (0) present; (1) absent.
6. Premaxilla, postero-medial region, dorsal surface, small projection: (0) absent; (1) present.
7. Premaxilla, lateral extremity, distinctive process: (0) absent; (1) present.
8. Maxilla, length relative to distance between mesethmoid cornua: (0) equal or slightly longer; (1) about one time and half; (2) about twice or slightly more.
9. Autopalatine, general shape: (0) slender, with well-developed postero-lateral process; (1) broad, postero-lateral process absent.
10. Autopalatine, posterior region, length relative to autopalatine length: (0) short, about half length or slightly less; (1) long, about two thirds.
11. Autopalatine, postero-lateral process, posterior portion, expansion: (0) absent; (1) present.
12. Autopalatine, postero-lateral tip, narrow and flat ossification postero-medially directed: (0) absent; (1) present.
13. Autopalatine, postero-medial margin, latero-dorsally directed process: (0) absent; (1) present.
14. Autopalatine, anterior cartilage head, anterior margin, ossification: (0) absent; (1) present.
15. Autopalatine, osseous portion, anterior margin, shape: (0) slightly curved to about straight; (1) strongly sinuous.

16. Antorbital, shape: (0) rod-shaped; (1) comma-shaped.
17. Supraorbital, development: (0) well-developed; (1) rudimentary.
18. Metapterygoid, development: (0) well-developed; (1) rudimentary.
19. Hyomandibula, dorsal margin, area just anterior to cartilage articulating hyomandibula and neurocranium, prominent expansion: (0) absent; (1) present.
20. Quadrate, dorsal process, posterior margin, laminar extension: (0) absent; (1) present.
21. Opercle, odontode patch, width relative to length of cartilage articulating hyomandibula and neurocranium: (0) smaller; (1) larger.
22. Opercle, dorsal surface, area just anterior to odontode patch: (0) straight to slightly concave; (1) with prominent concavity.
23. Interopercle, area between dorsal process and odontode patch, shape: (0) not constricted; (1) strongly constricted.
24. Interopercle, odontode patch, length relative to width of opercular odontode patch: (0) equal or smaller; (1) about twice larger.
25. Interopercle, lateral surface, projection: (0) absent; (1) present.
26. Neurocranium, roof, dorsal surface; aperture: (0) with open fontanel (1) roof solid, without apertures.
27. Neurocranium, antero-frontal, lateral constriction: (0) gradual and weak; (1) abrupt and strong.
28. Neurocranium, frontal, anterior extent relative to autopalatine structures: (0) posterior to articular facet for lateral ethmoid; (1) near postero-medial tip overlapping vomer; (2) about mid-length between postero-medial tip and limit between osseus portion and anterior cartilage.
29. Neurocranium, anterior supraorbital canal (between pores s1–s3): (0) present; (1) absent.
30. Neurocranium, posterior supraorbital canal (between pores s3–po1): (0) present; (1) absent.
31. Neurocranium, supraorbital pore s6: (0) paired; (1) single, median.
32. Ceratobranchial 4, sub-proximal region, process: (0) present; (1) absent.
33. Hypobranchial 3, ossification: (0) with well-developed anterior ossification; (1) ossification rudimentary, usually absent.
34. Parurohyal, lateral process, shape: (0) short and broad; (1) long and narrow.
35. Ribs, number: (0) six or more; (1) four or fewer (taken from Costa & Bockmann [6]).
36. Trunk, pigmentation: (0) well pigmented, making body wall opaque; (1) hyaline, with a few scattered chromatophores.
37. Trunk, shape: (0) fusiform; (1) eel-like.
38. Trunk, precaudal vertebrae, neural spines, anterior process: (0) present; (1) absent.
39. Trunk, dorsal surface, pre-dorsal region, adipose fold: (0) absent; (1) present.
40. Caudal peduncle, procurrent caudal-fin rays, anterior extent: (0) limited to area close to caudal fin; (1) anteriorly extending to near dorsal and anal fins.
41. Caudal skeleton, dorsal and ventral hypural plates, fusion: (0) unfused, separated by broad gap; (1) partially fused, at least with posterior gap separating plates; (2) fused, often resting small antero-middle notch.
42. Caudal skeleton, lower hypurals, shape: (0) subtrapezoidal; (1) subrectangular as a result of an anteroventral expansion. Remarks: In taxa with the character state 1, the ventral lobe of the caudal fin is slightly expanded posteriorly and there is a reduced number (4–7) of ventral procurrent caudal-fin rays, apomorphic conditions here considered as possibly interdependent, thus not analysed separately.
43. Caudal fin, general morphology: (0) subtruncate; (1) rounded, almost indistinct between caudal peduncle procurrent rays; (2) bilobed.
44. Caudal fin, principal caudal-fin rays, number: (0) 17; (1) 13; (2) 11 or 12.
45. Pectoral girdle, main components (cleithrum and proximal radials), development: (0) robust and thick; (1) narrow and thin.
46. Pectoral fin, rays, development: (0) first and remaining rays well developed; (1) first rays developed, followed by one to three rudimentary rays; (2) single barbel-like rayed.

47. Pectoral fin, first ray, length relative to subsequent rays: (0) slightly longer; (1) shorter. Remarks: the taxa having a relatively short and robust first pectoral-fin ray (character state 1), also have a hypertrophied major proximal radial, considered to be dependent conditions of a single event.
48. Pectoral fin, first ray, tip, filament, length relative to pectoral fin length: (0) short, 20% or less; (1) long, about 70–80%.
49. Pectoral fin, minor proximal radial, ossification: (0) cartilaginous; (1) ossified.
50. Pelvic fin, medial interspace: (0) in close proximity; (1) broader than pelvic-fin base; (?) taxa without pelvic fin.
51. Pelvic fin: (0) present; (1) absent.
52. Dorsal fin: (0) present; (1) absent.
53. Anal fin, origin, position relative to principal dorsal-fin rays: (0) posteriorly placed, in vertical through or posterior to them; (1) anteriorly placed, in vertical anterior to them.
54. Nasal barbel, development: (0) well-developed, reaching between opercular odontode patch and pectoral fin base; (1) rudimentary, barely reaching posterior nostril.
55. Eye, position in head: (0) anterior; (1) posterior.
56. Eye, size expressed as percentage of head length: (0) medium sized (about 12–16%); (1) hypertrophied (about 18–22%); (2) minute (about 7–10%).
57. Head, ventral surface, branchiostegal region, paired barbel-like short projection: (0) absent; (1) present.

Appendix D

Matrix of distribution of character states among taxa.

Trichogenes longipinnis	000000000000000000000001000000001000000000100000000?0000
Ituglanis boitata	000000000000000000001001010000000000000000010000000000000
Trichomycterus nigricans	000000000000000000000001000000000000000000010000000000000
Scleronema minutum	000000010000000000001000001000?000000000000100100100001000
Homodiaetus anisitsi	0?000000000000?100000000010?011110000000100000000001000
Stauroglanis gouldingi	000001010000010001000000001010000111000000010000000000100
Pygidianops amphioxus	??000001000000?100000?01001??001111010????0???0?11?0??0
Microcambeva filamentosa	000101010000001001101100100010110111001000110001000002000
Microcambeva ribeirae	000101020100000001001100101010110111000001110010110001111
Microcambeva bendego	000101020100000001001100101010110111000001110010110001111
Microcambeva barbata	000101120000011001001000100010010111000001110000110000111
Microcambeva watu	00010112001001100100100?000100101110?000111000011000111
Microcambeva jucuensis	000101120010011001001000100010010111000001110000110000111
Microcambeva mucuriensis	000101120010011001001000100010010111000001110000110000111
Microcambeva draco	000101120010011001001000100010010111000001110000110000111
Listrura tetraradiata	100111001001101111000011110111?011101101202110000?1000020
Listrura nematoptetyx	102111001001001111010010110211?011101101202212000?1010020
Listrura macacuensis	10211100100100111101001011021 1?011101101202212 0?0?1010020
Listrura sp. 2	??????????????????????????2?????????????????2????11?????
Listrura macaensis	102111001001001111010010110211?011101101202212 0?0?1010020
Listrura costai	102111001001001111010010110211?011101101202212 0?0?1010020
Listrura picinguabae	112111001001001111010010110211?011101101202212 0?0?1010020
Listrura camposi	101111001001001111000010110111?011101101102211 0?0?1000020
Listrura sp. 1	101111001001001111000010110111?011101101102211 0?0?1000020
Listrura depinnai	101111001001001111000010110111?011101101102211 0?0?11?0020

Appendix E

Best-fitting models.

Partition	Base Pairs	Evolutive Model
COI 1st	219	TNe+G4
COI 2nd	218	F81+F+I
COI 3rd	219	TIM+F+I+G4
CYTB 1st	361	TNe+G4
CYTB 2nd	362	HKY+F
CYTB 3rd	361	TN+F+G4
RAG2 1st	274	TIM2e+I
RAG2 2nd	275	K2P+I
RAG2 3rd	275	HKY+F+I
Morphology	57	JC+I+G4

References

1. McConnell, R.; Lowe-McConnell, R.H. *Ecological Studies in Tropical Fish Communities*; Cambridge University Press: Cambridge, UK, 1987.
2. Myers, N.; Mittermeir, R.A.; Mittermeir, C.G.; Da Fonseca, G.A.B.; Kent, J. Biodiversity hotspots for conservation priorities. *Nature* **2000**, *403*, 853–858. [CrossRef] [PubMed]
3. Costa, W.J.E.M.; Henschel, E.; Katz, A.M. Multigene phylogeny reveals convergent evolution in small interstitial catfishes from the Amazon and Atlantic forests (Siluriformes: Trichomycteridae). *Zool. Scr.* **2020**, *49*, 159–173. [CrossRef]
4. De Pinna, M.C.C. A new genus of trichomycterid catfish (Siluroidei, Glanapteryginae), with comments on its phylogenetic relationships. *Rev. Suisse de Zool.* **1988**, *95*, 113–128. [CrossRef]
5. Costa, W.J.E.M.; Bockmann, F.A. A new genus and species of Sarcoglanidinae (Siluriformes: Trichomycteridae) from southeastern Brazil, with a re-examination of subfamilial phylogeny. *J. Nat. Hist.* **1994**, *28*, 715–730. [CrossRef]
6. Costa, W.J.E.M.; Bockmann, F.A. Un nouveau genre néotropical de la famille des Trichomycteridae (Siluriformes: Loricarioidei). *Rev. Fr. d'Aquariologie Herpétologie* **1993**, *20*, 43–46.
7. Villa-Verde, L.; Costa, W.J.E.M. A new glanapterygine catfish of the genus *Listrura* (Siluriformes: Trichomycteridae) from the southeastern Brazilian coastal plains. *Zootaxa* **2006**, *1142*, 43–50. [CrossRef]
8. Landim, M.I.; Costa, W.J.E.M. *Listrura tetraradiata* (Siluriformes: Trichomycteridae): A new glanapterygine catfish from the southeastern Brazilian coastal plains. *Copeia* **2002**, *2002*, 152–156. [CrossRef]
9. De Pinna, M.C.C.; Wosiacki, W. A new interstitial catfish of the genus *Listrura* from southern Brazil (Siluriformes, Trichomycteridae, Glanapteryginae). *Proc. Biol. Soc. Wash.* **2002**, *115*, 720–726.
10. Villa-Verde, L.; Lazzarotto, H.; Lima, S.Q.M. A new glanapterygine catfish of the genus *Listrura* (Siluriformes: Tricho-mycteridae) from southeastern Brazil, corroborated by morphological and molecular data. *Neotrop. Ichthyol.* **2012**, *10*, 527–538. [CrossRef]
11. Villa-Verde, L.; Ferrer, J.; Malabarba, L.R. A New Species of *Listrura* from Laguna dos Patos System, Brazil: The Southernmost Record of the Glanapteryginae (Siluriformes: Trichomycteridae). *Copeia* **2013**, *2013*, 641–646. [CrossRef]
12. Costa, W.J.E.M.; Lima, S.M.Q.; Bizerril, R.S. *Microcambeva ribeirae* sp. n. (Teleostei: Siluriformes: Trichomycteridae): A New Sarcoglanidine Catfish from the Rio Ribeira do Iguape Basin, Southeastern Brazil. *Zootaxa* **2004**, *563*, 1–10. [CrossRef]
13. Mattos, J.L.; Lima, S.M.Q. *Microcambeva draco*, a new species from north-eastern Brazil (Siluriformes: Trichomycteridae). *Ichthyol. Explor. Freshw.* **2010**, *21*, 233–238.
14. Costa, W.J.E.M.; Katz, A.M.; Mattos, J.L.O.; Rangel-Pereira, F.S. Two new species of miniature psammophilic sarcoglanidine catfishes of the genus *Microcambeva* from the Atlantic Forest of eastern Brazil (Siluriformes: Trichomycteridae). *J. Nat. Hist.* **2019**, *53*, 1837–1851. [CrossRef]
15. De Medeiros, L.S.; Moreira, C.R.; de Pinna, M.C.C.; Lima, S.M.Q. A new catfish species of *Microcambeva* Costa & Bockmann 1994 (Siluriformes: Trichomycteridae) from a coastal basin in Rio de Janeiro State, southeastern Brazil. *Zootaxa* **2020**, *4895*, 111–123.
16. De Medeiros, L.S.; Sarmento-Soares, L.M.; Lima, S.M.Q. A new psammophilous catfish of the genus *Microcambeva* (Teleostei: Trichomycteridae) from the Rio Doce basin, southeastern Brazil. *Ichthyol. Explor. Freshw.* **2021**, 1–13. [CrossRef]
17. Costa, W.J.; Vilardo, P.; Katz, A.M. Sympatric sister species with divergent morphological features of psammophilic catfishes of the southeastern Brazilian genus *Microcambeva* (Siluriformes: Trichomycteridae). *Zool. Anz.* **2020**, *285*, 12–17. [CrossRef]

18. Costa, W. Comparative Osteology, Phylogeny and Classification of the Eastern South American Catfish Genus *Trichomycterus* (Siluriformes: Trichomycteridae). *Taxonomy* **2021**, *1*, 160–191. [CrossRef]
19. Costa, W.J.E.M. Description de huit nouvelles espèces du genre *Trichomycterus* (Siluriformes: Trichomycteridae), du Brésil oriental. *Rev. Fr. d'Aquariologie Herpetol.* **1992**, *18*, 101–110.
20. Costa, W.J.E.M.; Katz, A.M.; Mattos, J.L.O.; Amorim, P.F.; Mesquita, B.O.; Vilardo, P.J.; Barbosa, M.A. Historical review and redescription of three poorly known species of the catfish genus *Trichomycterus* from south-eastern Brazil (Siluriformes: Trichomycteridae). *J. Nat. Hist.* **2020**, *53*, 2905–2928. [CrossRef]
21. Taylor, W.R.; Van Dyke, G.C. Revised procedures for staining and clearing small fishes and other vertebrates for bone and cartilage study. *Cybium* **1985**, *9*, 107–119.
22. Costa, W.J.E.M.; Katz, A.M. Integrative taxonomy supports high species diversity of south-eastern Brazilian mountain catfishes of the *T. reinhardti* group (Siluriformes: Trichomycteridae). *Syst. Biodivers.* **2021**, *19*, 601–621. [CrossRef]
23. Arratia, G.; Huaquin, L. Morphology of the lateral line system and of the skin of diplomystic and certain primitive loricarioid catfishes and systematic and ecological considerations. *Bonn Zool. Monogr.* **1995**, *36*, 1–110.
24. Bockmann, F.A.; Casatti, L.; de Pinna, M.C.C. A new species of trichomycterid catfish from the Rio Paranapanema, southeastern Brazil (Teleostei; Siluriformes), with comments on the phylogeny of the family. *Ichthyol. Explor. Freshw.* **2004**, *15*, 225–242.
25. Hardman, M.; Page, L.M. Phylogenetic relationships among bullhead catfishes of the genus *Ameiurus* (Siluriformes: Ictaluridae). *Copeia* **2003**, *2003*, 20–33. [CrossRef]
26. Ward, R.D.; Zemlak, T.S.; Innes, B.H.; Last, P.R.; Hebert, P. DNA barcoding Australia's fish species. *Philos. Trans. R. Soc. B Biol. Sci.* **2005**, *360*, 1847–1857. [CrossRef] [PubMed]
27. Chenna, R. Multiple sequence alignment with the Clustal series of programs. *Nucleic Acids Res.* **2003**, *31*, 3497–3500. [CrossRef] [PubMed]
28. Kumar, S.; Stecher, G.; Tamura, K. MEGA7: Molecular evolutionary genetics analysis version 7.0 for bigger datasets. *Mol. Biol. Evol.* **2016**, *33*, 1870–1874. [CrossRef]
29. Sereno, P.C. Logical basis for morphological characters in phylogenetics. *Cladistics* **2007**, *23*, 565–587. [CrossRef]
30. Kalyaanamoorthy, S.; Minh, B.Q.; Wong, T.; Von Haeseler, A.; Jermiin, L.S. ModelFinder: Fast model selection for accurate phylogenetic estimates. *Nat. Methods* **2017**, *14*, 587–589. [CrossRef]
31. Nguyen, L.-T.; Schmidt, H.; Von Haeseler, A.; Minh, B.Q. IQ-TREE: A Fast and Effective Stochastic Algorithm for Estimating Maximum-Likelihood Phylogenies. *Mol. Biol. Evol.* **2015**, *32*, 268–274. [CrossRef]
32. Chernomor, O.; Von Haeseler, A.; Minh, B.Q. Terrace Aware Data Structure for Phylogenomic Inference from Supermatrices. *Syst. Biol.* **2016**, *65*, 997–1008. [CrossRef]
33. Guindon, S.; Dufayard, J.F.; Lefort, V.; Anisimova, M.; Hordijk, W.; Gascuel, O. New algorithms and methods to estimate maximum-likelihood phylogenies: Assessing the performance of PhyML 3.0. *Syst. Biol.* **2010**, *59*, 307–321. [CrossRef] [PubMed]
34. Anisimova, M.; Gil, M.; Dufayard, J.F.; Dessimoz, C.; Gascuel, O. Survey of branch support methods demonstrates accuracy, power, and robustness of fast likelihood-based approximation schemes. *Syst. Biol.* **2011**, *60*, 685–699. [CrossRef] [PubMed]
35. Minh, B.Q.; Nguyen, M.A.T.; Von Haeseler, A. Ultrafast Approximation for Phylogenetic Bootstrap. *Mol. Biol. Evol.* **2013**, *30*, 1188–1195. [CrossRef]
36. Hoang, D.T.; Chernomor, O.; Von Haeseler, A.; Minh, B.Q.; Vinh, L.S. UFBoot2: Improving the Ultrafast Bootstrap Approximation. *Mol. Biol. Evol.* **2017**, *35*, 518–522. [CrossRef] [PubMed]
37. Goloboff, P.A.; Farris, J.S.; Nixon, K.C. TNT, a free program for phylogenetic analysis. *Cladistics* **2008**, *24*, 774–786. [CrossRef]
38. Felsenstein, J. Confidence limits on phylogenies: An approach using the bootstrap. *Evolution* **1985**, *39*, 783–791. [CrossRef]
39. Anoop, V.; Britz, R.; Arjun, C.; Dahanukar, N.; Raghavan, R. *Pangio bhujia*, a new, peculiar species of miniature subterranean eel loach lacking dorsal and pelvic fins from India (Teleostei: Cobitidae). *Zootaxa* **2019**, *4683*, 144–150. [CrossRef]
40. Britz, R.; Doherty-Bone, T.M.; Kouete, M.T.; Sykes, D.; Gower, D.J. *Monopterus luticolus*, a new species of swamp eel from Cameroon (Teleostei: Synbranchidae). *Ichthyol. Explor. Freshw.* **2016**, *27*, 309–323.
41. De Pinna, M.; Zuanon, J.; Py-Daniel, L.R.; Petry, P. A new family of neotropical freshwater fishes from deep fossorial Amazonian habitat, with a reappraisal of morphological characiform phylogeny (Teleostei: Ostariophysi). *Zool. J. Linn. Soc.* **2018**, *182*, 76–106. [CrossRef]
42. Yamada, T.; Sugiyama, T.; Tamaki, N.; Kawakita, A.; Kato, M. Adaptive radiation of gobies in the interstitial habitats of gravel beaches accompanied by body elongation and excessive vertebral segmentation. *BMC Evol. Biol.* **2009**, *9*, 145. [CrossRef] [PubMed]
43. Adriaens, D.; Baskin, J.N.; Coppens, H. Evolutionary morphology of trichomycterid catfishes: About hanging on and digging in. In *Origin and Phylogenetic Interrelationships of Teleosts*; Nelson, J.S., Schultze, H.P., Wilson, M.V.H., Eds.; Verlag Dr. Friedrich Pfeil: München, Germany, 2010; pp. 337–362.
44. Wagner, M.; Bračun, S.; Skofitsch, G.; Kovačić, M.; Zogaris, S.; Iglésias, S.; Sefc, K.M.; Koblmüller, S. Diversification in gravel beaches: A radiation of interstitial clingfish (Gouania, Gobiesocidae) in the Mediterranean Sea. *Mol. Phylogenetics Evol.* **2019**, *139*, 106525. [CrossRef]
45. Villa-Verde, L.; Britto, M.R.; Abilhoa, V. Novos exemplares de *Listrura boticario* de Pinna & Wosiacki (Siluriformes: Trichomycteridae). *Bol. Soc. Bras. de Ictiol.* **2008**, *91*, 5–6.

46. Villa-Verde, L.; Lima, S.M.Q.; Carvalho, P.H.; de Pinna, M.C.C. Rediscovery, taxonomic status and conservation of the threatened catfish *Listrura camposi* (Miranda-Ribeiro) (Siluriformes: Trichomycteridae). *Neotrop. Ichthyol.* **2013**, *11*, 55–64. [CrossRef]
47. Nico, L.G.; de Pinna, M.C.C. Confirmation of *Glanapteryx anguilla* (Siluriformes, Trichomycteridae) in the Orinoco River basin, with notes on the distribution and habitats of the Glanapteryginae. *Ichthyol. Explor. Freshw.* **1996**, *7*, 27–32.
48. De Almeida-Val, V.M.F.; Fé, L.M.L.; de Campos, D.F. Evolutionary aspects on the comparative biology of lungfishes: Emphasis on South-American Lungfish, *Lepidosiren paradoxa*. In *Phylogeny, Anatomy and Physiology of Ancient Fishes*; Zaccone, G., Dabrowski, K., Hedrick, M.S., Fernandes, J.M.O., Icardo, J.M., Eds.; CRC Press: Boca Raton, FL, USA, 2016; pp. 38–56.
49. Zuanon, J.; Bockmann, F.A.; Sazima, I. A remarkable sand-dwelling fish assemblage from central Amazonia, with comments on the evolution of psammophily in South American freshwater fishes. *Neotrop. Ichthyol.* **2006**, *4*, 107–118. [CrossRef]
50. Zuanon, J.; Sazima, I. Natural history of *Stauroglanis gouldingi* (Siluriformes: Trichomycteridae), a miniature sand-dwelling candiru from central Amazonia streamlets. *Ichthyol. Explor. Freshw.* **2004**, *15*, 201–208.
51. Baskin, J.N. *Structure and Relationships of the Trichomycteridae*; City University of New York: New York, NY, USA, 1973. Supplementary material of de Pinna. *Neotrop. Ichthyol.* **2016**, *14*, S1–S62.
52. De Pinna, M.C.C. A new sarcoglandine catfish, phylogeny of its subfamily, and an appraisal of the phyletic status of the Trichomycterinae (Teleostei, Trichomycteridae). *Am. Mus. Novit.* **1989**, *2950*, 1–39.
53. Myers, G.S.; Weitzman, S.H. Two remarkable new trichomycterid catfishes from the Amazon basin in Brazil and Colombia. *J. Zool.* **1966**, *149*, 277–287. [CrossRef]
54. Costa, W.J.E.M. A new genus and species of Sarcoglanidinae (Siluriformes: Trichomycteridae) from the Araguaia basin, central Brazil, with notes on subfamilial phylogeny. *Ichthyol. Explor. Freshw.* **1994**, *5*, 207–216.
55. Henschel, E.; Katz, A.M.; Costa, W.J.E.M. A new candiru of the genus *Paracanthopoma* (Siluriformes: Trichomycteridae) from the Araguaia River basin, Central Brazil. *J. Fish Biol.* **2021**, in press. [CrossRef]
56. Schaefer, S.A.; Provenzano, F.; de Pinna, M.; Baskin, J.N. New and noteworthy Venezuelan glanapterygine catfishes (Siluriformes, Trichomycteridae), with discussion of their biogeography and psammophily. *Am. Mus. Novit.* **2005**, *3496*, 1–27. [CrossRef]
57. Near, T.J.; Dornburg, A.; Eytan, R.I.; Keck, B.P.; Smith, W.L.; Kuhn, K.L.; Moore, J.A.; Price, S.A.; Burbrink, F.T.; Friedman, M.; et al. Phylogeny and tempo of diversification in the superradiation of spiny-rayed fishes. *Proc. Natl. Acad. Sci. USA* **2013**, *110*, 12738–12743. [CrossRef]
58. Betancur-R, R.; Ortí, G.; Pyron, R.A. Fossil-based comparative analyses reveal ancient marine ancestry erased by extinction in ray-finned fishes. *Ecol. Lett.* **2015**, *18*, 441–450. [CrossRef] [PubMed]
59. De Pinna, M.C.C. Phylogenetic relationships of neotropical Siluriformes (Teleostei: Ostariophysi): Historical overview and synthesis of hypotheses. In *Phylogeny and Classification of Neotropical Fishes*; Malabarba, L.R., Reis, R.E., Vari, R.P., Lucena, Z.M.S., Lucena, C.A.S., Eds.; Edipucrs: Porto Alegre, Brazil, 1998; pp. 279–330.
60. Sullivan, J.P.; Lundberg, J.G.; Hardman, M. A phylogenetic analysis of the major groups of catfishes (Teleostei: Siluriformes) using rag1 and rag2 nuclear gene sequences. *Mol. Phylogenetics Evol.* **2006**, *41*, 636–662. [CrossRef] [PubMed]